# Zero-range potential model for the description of atomic and molecular systems in a laser field

P. S. Krstić
*Institute of Physics, P.O. Box 57, 11001 Belgrade, Yugoslavia*

D. B. Milošević
*Research and Development Department, "Zrak," Adema Buće 96, 71000 Sarajevo, Yugoslavia*

R. K. Janev
*Institute of Physics, P.O. Box 57, 11001 Belgrade, Yugoslavia*
(Received 20 August 1990)

The method of zero-range potential is used to model negative atomic and quasimolecular ions in a circularly polarized laser field. The range of the laser-field parameters is extended in comparison with the previous calculations of the complex quasienergies of an atomic particle. A closed-form expression that defines the adiabatic electronic complex quasienergies of a two-state quasimolecular system is derived and solved numerically. Both laser-induced widths and shifts of the terms are discussed for a wide region of the laser-field parameters and internuclear distances, using $H_2^-$ and $OH^-$ ions as examples. The effect of suppression of the ionization rate of the excited state of a negative quasimolecular ion at small internuclear distances due to the presence of a laser field, as well as deepening of the ground-term potential well, was found.

## I. INTRODUCTION

In the analysis of atomic and molecular processes in a strong laser field, various unperturbative methods have limited bounds of validity, which are often difficult to determine in terms of both the laser field parameters (radiation intensity, frequency, polarization) and the atomic (molecular) system parameters. Therefore, the models of an atomic (molecular)system that enable an analytical solution of the problem could provide both important information on applicability of the approximations and predictions of new effects. An electron in the presence of one three-dimensional (3D) attractive zero-range potential (ZRP, a $\delta$ function), embedded in a laser field, is so far the only known exactly solvable three-dimensional model for the description of the behavior of an atomic system in a laser field [1-5].

The problem of one ZRP in an elliptically polarized laser field cannot be solved exactly. However, if the field is circularly polarized, transformation to the referent system which rotates with the radiation-field frequency $\omega$ simplifies the problem to an exactly solvable time-independent one [1-5]. On the other hand, a model of two (or more) ZRP's in the absence of the laser field has been successfully applied to a negative molecular ion system to describe the processes occurring in negative-ion–atom (–molecule) collisions and in the electron-molecule scattering [6-8]. Furthermore, one can construct a class of 3D, exactly solvable models which describe a particle that interacts with a few centers [9]. ZRP and the 3D Kronig-Penny model [10] are two well-known examples of this class. A one-dimensional model of a negative molecular ion in the presence of a laser field, defined by two $\delta$ functions has been treated earlier [11].

In this paper we present a nearly exactly soluble 3D model of a negative diatomic molecular ion in a laser field. The eigenvalue Floquet-type problem is solved in the closed form for the two ZRP embedded in a circularly polarized laser field of arbitrary intensity (Sec. II). The standard semiclassical approach of internuclear motion is adopted [12] resulting in a time-dependent Schrödinger equation for the electron motion, where the internuclear distance $R$ is a known function of time. Assuming $R$ fixed, the problem in a circularly polarized laser field can be reduced to a time-independent one. The real parts of the obtained complex quasienergies at different $R$ then represent adiabatic quasimolecular terms, while the imaginary parts correspond to their widths due to the decay of the system into the quasimolecular continuum. The $H_2^-$ and $OH^-$ molecular systems are treated in detail. The generalization of the procedure to an analogous model for three and more atom molecules is straightforward and will not be pursued here. In order to present the employed method in a clearer fashion, as well as to extract those laser-field effects which are at least qualitatively independent on the quasimolecular nature of the system, the eigenvalue problem of one ZRP in a laser field is also discussed (Sec. II). The range of the laser-field parameters is extended in comparison with the previous calculations [1-5] of the complex quasienergies.

The quantum electrodynamics (QED) formalism of the radiation field and the "laser approximation" are used, which give results equivalent to those obtained with the classical radiation field. The vector potential of an elliptically polarized laser field of frequency $\omega$, wave vector $\mathbf{k}=\omega\hat{\mathbf{k}}$, and polarization angle $\kappa$ are defined by

$$\mathbf{A}(\mathbf{r})=\frac{A_0}{2N^{1/2}}(A_1^{(+)}\mathbf{\Lambda}_1+iA_1^{(-)}\mathbf{\Lambda}_2)\ , \tag{1.1a}$$

where

 

$$A_1^{(\pm)}=ae^{i\mathbf{k}\cdot\mathbf{r}}\pm a^{\dagger}e^{-i\mathbf{k}\cdot\mathbf{r}} ,$$
$$\Lambda_1=\hat{\mathbf{e}}_1\cos(\kappa) , \tag{1.1b}$$
$$\Lambda_2=\hat{\mathbf{e}}_1\sin(\kappa) .$$

$A_0$ is the classical amplitude of the vector potential with $N$ photons in the quantization volume.

The state vector $|\Psi(t)\rangle$ satisfies the time-dependent Schrödinger equation for an electron in the presence of both the laser field and potential $V(r)$,

$$i\frac{\partial}{\partial t}|\Psi(t)\rangle=H|\Psi(t)\rangle , \tag{1.2}$$

where $H=H_L+V$ and $H_L$ is the Hamiltonian of an electron in the laser field, defined in Appendix A. It was shown by Shakeshaft [13] that, in the wave-packet representation, if the condition

$$\Gamma\ll\varepsilon_{\mu_0}=\varepsilon_0-U_p+\Delta+\mu_0\omega<\omega \tag{1.3}$$

is fulfilled, $|\Psi(t)\rangle$ is given by

$$|\Psi(t)\rangle\cong\exp(-i\tilde{E}t)|\Psi_{\tilde{E}}(\mathbf{r})\rangle , \tag{1.4a}$$

where

$$\tilde{E}=\varepsilon_0+\Delta+N\omega-\frac{i}{2}\Gamma . \tag{1.4b}$$

In Eq. (1.3), $\mu_0$ is the minimum number of photon to ionize from a bound state with energy $\varepsilon_0$ and $U_p=e^2A_0^2/(4m)$ is the laser-field ponderomotive potential. The initial energy of the system, $\varepsilon_0+N\omega$, is shifted by $\Delta$ and has the lifetime $1/\Gamma$ (i.e., the width $\Gamma$). $\varepsilon_\mu$ is the energy of the electron after absorbing $\mu$ photons in the bound state.

According to Eqs. (1.2) and (1.4a), $|\Psi_{\tilde{E}}(\mathbf{r})\rangle$ satisfies the stationary Schrödinger equation with complex energy $\tilde{E}$, $H|\Psi_{\tilde{E}}(\mathbf{r})\rangle=\tilde{E}|\Psi_{\tilde{E}}(\mathbf{r})\rangle$, which can be written in the integral form as

$$|\Psi_{\tilde{E}}(\mathbf{r})\rangle=\int d\mathbf{r}'G_L(\tilde{E};\mathbf{r},\mathbf{r}')V(\mathbf{r}')|\Psi_{\tilde{E}}(\mathbf{r}')\rangle , \tag{1.5a}$$

where $G_L$ is the Volkov Green's operator, defined by

$$(E-H_L)G_L(E;\mathbf{r},\mathbf{r}')=\delta(\mathbf{r}-\mathbf{r}') \tag{1.5b}$$

with outgoing-wave boundary conditions (Appendix A). $|\Psi_{\tilde{E}}(\mathbf{r})\rangle$ are the vectors in the photon space. In the phase representation, and within the laser approximation, Eq. (1.5a) can be written in the form

$$\Psi_{\tilde{E}}(\mathbf{r},\vartheta)=-\frac{m}{(2\pi)^2}\int_0^{2\pi}d\vartheta'\int d\mathbf{r}'e^{i\Phi(\mathbf{r},\vartheta;\mathbf{r}',\vartheta')}\sum_\nu e^{i(N-\nu)(\vartheta-\vartheta')}\frac{\exp[ik_\nu(\tilde{E})|\mathbf{r}-\mathbf{r}'-\mathbf{f}(\mathbf{r},\vartheta;\mathbf{r}',\vartheta')|]}{|\mathbf{r}-\mathbf{r}'-\mathbf{f}(\mathbf{r},\vartheta;\mathbf{r}',\vartheta')|}V(\mathbf{r}')\Psi_{\tilde{E}}(\mathbf{r}',\vartheta) \tag{1.6a}$$

or, equivalently, as

$$\Psi_{\tilde{E}}(\mathbf{r},\vartheta)=-\frac{i}{\omega}\int d\mathbf{r}'\int_0^\infty dx\left[\frac{m\omega}{2\pi ix}\right]^{3/2}e^{ix(\tilde{E}-U_p)/\omega}$$
$$\times\exp\left[i\left[\Phi(\mathbf{r},\vartheta;\mathbf{r}',\vartheta-x)+\frac{m\omega}{2x}[\mathbf{r}-\mathbf{r}'-\mathbf{f}(\mathbf{r},\vartheta;\mathbf{r}',\vartheta-x)]^2\right]\right]V(\mathbf{r}')\Psi_E(\mathbf{r}',\vartheta-x) , \tag{1.6b}$$

where $\phi$, $k_\nu$, and $\mathbf{f}$ are defined in Appendix A.

The integral equations in the "photon representation" can be obtained from Eqs. (1.6) with the use of

$$\Psi_{\tilde{E},m}(\mathbf{r})=\langle N-m|\Psi_{\tilde{E}}(\mathbf{r})\rangle$$
$$=\frac{1}{(2\pi)^{1/2}}\int_0^{2\pi}d\vartheta\,e^{-i(N-m)\vartheta}\Psi_{\tilde{E}}(\mathbf{r},\vartheta) . \tag{1.7}$$

Imposing the boundary conditions of the zero-range potentials, a closed-form expression for the complex energies $\tilde{E}$ will be obtained from Eqs. (1.6) in Sec. II. It should be mentioned that Eqs. (1.5)–(1.7) are more general than the corresponding Berson's result [2] because Eqs. (1.5)–(1.7) can be applied to both an elliptically polarized laser field and to an arbitrary potential $V(r)$ (which defines an atomic or a molecular system).

Before we start to apply the above consideration to the ionization of an atomic and molecular negative-ion system, it is useful to briefly discuss the model of the zero-range potential and its relation to a real system [6-8,14]. An electron in one ZRP is a prominent example of a model of an atomic negative ion, with the valence electron in an $s$ state [8,14]. The binding energy $|\varepsilon_0|$ of the outer electron is significantly smaller than those of the other bound electrons in the ion. Therefore, the wave function of that electron occupies a much larger domain in space than the range where the binding potential is significant (i.e., the outer electron spends most of the time outside the potential well). In the ZRP model, the electron is considered as being free with the influence of the potential on its motion taken into account through a boundary condition on its wave function at the coordinate origin. The problem is thus reduced to the solution of the Schrödinger equation for a free $s$-state electron, subjected to the boundary condition

$$(r\varphi)^{-1}\frac{d}{dr}(r\varphi)\bigg|_{r=0}=-\kappa_0,\quad \varepsilon_0=-\frac{\kappa_0^2}{2m} . \tag{1.8}$$

The wave function of the only bound state is then

$$\varphi(r)=B(\kappa_0/2\pi)^{1/2}\frac{e^{-\kappa_0 r}}{r} , \tag{1.9}$$

where $B$ is the normalization factor which is equal to 1

within the model. It can be also found from the variational calculations in order to fit the real system of finite effective range.

A negative diatomic molecular ion in the $s$ state can be described by a model in which an electron at $\mathbf{r}$ moves in the field of two ZRP's, positioned at $\mathbf{R}_1$ and $\mathbf{R}_2$, respectively [6-8]. Assuming that the motion of the nuclei is defined by a given function of time, $R=R(t)=|\mathbf{R}_2-\mathbf{R}_1|$, and that this motion is adiabatically slow, the Schrödinger equation of the problem is reduced to

$$[E(R)-H_{\rm el}(\mathbf{r},\mathbf{R})]\Psi=0\ , \tag{1.10}$$

where $E(R)$ defines the adiabatic terms of the molecule, and $\mathbf{R}$ appears in Eq. (1.10) as a parameter. Similarly, as in the case of an atomic ion, the wave function of the outer electron in a molecular ion can be defined in the whole space (except at $\mathbf{R}_1$ and $\mathbf{R}_2$) as the one of the free particle with two boundary conditions of the form (1.8) at $\mathbf{r}=\mathbf{R}_1$ and $\mathbf{r}=\mathbf{R}_2$. So, at $\mathbf{r}=\mathbf{R}_j$, the boundary conditions similar to (1.8) are applied, with $\kappa_0\to\kappa_j$, $\varepsilon_0\to\varepsilon_{0j}$, where $\varepsilon_{0j}$ is the electron energy in the $j$th potential when the two ZRP's are at infinite distance. Then, the wave function of the electron can be represented as a linear combination of the solutions $\varphi_1$ and $\varphi_2$ of the type (1.9), i.e., $\psi(\mathbf{r})=c_1\varphi_1+c_2\varphi_2$, and applying the above boundary conditions, the equation for the eigenenergies follows in the form [6-8]

$$(\kappa-\kappa_1)(\kappa-\kappa_2)=\frac{\exp(-2\kappa R)}{R^2}\ . \tag{1.11}$$

If $R\geq R_g=(\kappa_1\kappa_2)^{-1/2}$, this equation has two real solutions for $\varepsilon(R)$—the bound states with $\varepsilon_2<\varepsilon_1\leq 0$ if $\varepsilon_{02}<\varepsilon_{01}$. If $R<R_g$, $\varepsilon_2$ stays negative, with $\lim_{R\to 0}(\varepsilon_2)=-\infty$. The singularity of $\varepsilon_2$ at $R\to 0$ is connected with the fact that, in this limit, the potentials are not independent and their mutual interaction has to be defined, as is done in Appendix B for a more general case (in the presence of the laser field). When $R<R_g$, the eigenenergy $\varepsilon_1$ of the excited state is complex ($\varepsilon_1=\mathrm{Re}\varepsilon_1-i\Gamma_R/2$), which corresponds to a quasistationary eigenstate of width $\Gamma_R$ [15]. Therefore, even in the absence of a laser field, the decay of the higher state of the quasimolecular negative ion is possible for a certain region of $R$.

The connection of the above-described model with a real molecular negative ion can be discussed, for instance, on the example of the $H_2^-$ ion. The binding energy of the $H^-$ ion is 0.7542 eV. The solutions of Eq. (1.11) yield adiabatic electronic terms of the $H_2^-$ molecule as functions of $R$ (Fig. 1), with $R_g=4.246a_B$. On the other hand, the molecular terms of $H_2^-$ have also been calculated by different methods—for example, by the variational method, or by the method of resonant states with complex local potentials, etc. [14]. The results of these methods can be used to identify the states, the energies of which are determined by the numerical solution of Eq. (1.11). The comparison as well as the symmetry considerations show that $\varepsilon_1$ and $\varepsilon_2$ correspond to terms of $^2\Sigma_g$ and $^2\Sigma_u$ symmetry [6], respectively, while the $^3\Sigma_u$ term of the $H_2$ molecule represents the referent energy level (horizontal axis at Fig. 1) of the terms of $H_2^-$. The two-ZRP model has led to excellent results for a detachment probability and the detached electron spectrum in ion-atom collision problems [14].

We note that the boundary condition (1.8) is equivalent to the choice of the local potential $V(r)$ in form

$$V(\mathbf{r})=\frac{2\pi}{m}\frac{1}{\kappa}\delta(\mathbf{r})\frac{\partial}{\partial r}r \tag{1.12}$$

and, in the case of a molecular ion, the outer electron moves in the system of two such potentials.

The numerical solutions for the complex quasienergies of an electron in one and two ZRP's in a circularly polarized laser field will be discussed in Sec. III. In Sec. IV, we give our concluding remarks. The system of units with $\hbar=c=1$ is used through out the text.

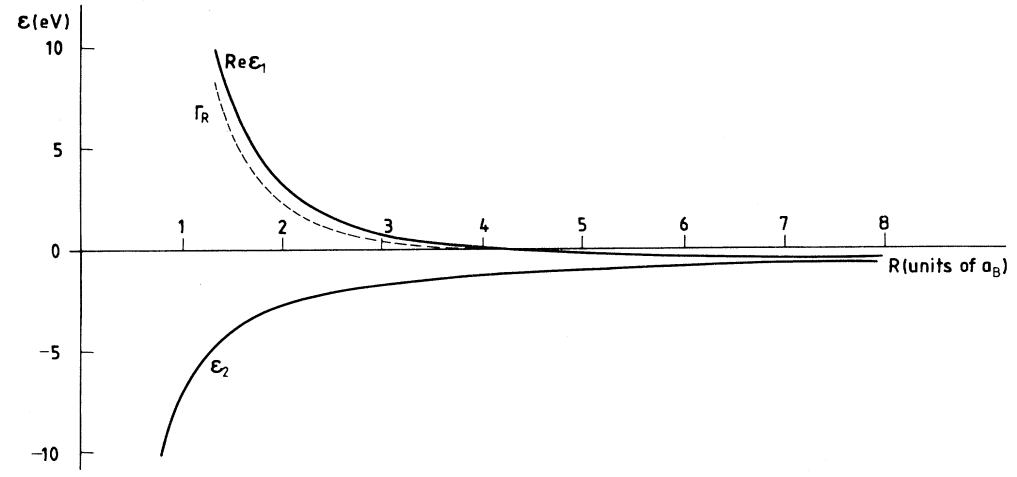


FIG. 1. Electronic terms of molecular ion $H_2^-$, obtained in the model of two ZRP's with $\varepsilon_{01}=\varepsilon_{02}=-0.7542$ eV. Interaction between two potential centers is not included (Appendix B).

## II. BASIC THEORY

The closed-form expression for the electron complex quasienergies of the ZRP model of a diatomic molecular negative ion is derived in this section. As a special case, the ZRP model of a negative atomic ion is also treated.

As was discussed in the Introduction, the eigenvalue problem is defined (at a fixed interpotential distance) by the time-independent Schrödinger equation

$$(\tilde{E}-H_L)|\psi_{\tilde{E}}(\mathbf{r},\mathbf{R})\rangle = \frac{2\pi}{m}\sum_{j=1}^{2}\frac{1}{\kappa_j}\delta(\mathbf{r}_j)\frac{\partial}{\partial r_j}r_j|\psi_{\tilde{E}}(\mathbf{r},\mathbf{R})\rangle \ , \quad (2.1)$$

where $\mathbf{r}_j=\mathbf{r}-\mathbf{R}_j$, $r_j=|\mathbf{r}_j|$, $j=1,2$. The boundary conditions of the type of (1.8) yield

$$\lim_{r_j\to 0}\frac{\partial}{\partial r_j}r_j|\Psi_{\tilde{E}}(\mathbf{r},\mathbf{R})\rangle=-\kappa_j|B_j\rangle, \quad j=1,2 \quad (2.2a)$$

or, equivalently,

$$\lim_{r_j\to 0}|\Psi_{\tilde{E}}(\mathbf{r},\mathbf{R})\rangle=\left[\frac{1}{r_j}-\kappa_j+O(r_j)\right]|B_j\rangle \ , \quad (2.2b)$$

where $|B_j\rangle$ is an arbitrary vector in the photon space

$$|B_j\rangle=\sum_{\nu}b_{j\nu}|N-\nu\rangle \ ,$$
$$\langle N-\nu|B_j\rangle=b_{j\nu} \ , \quad (2.2c)$$
$$\langle\vartheta|B_j\rangle=(2\pi)^{-1/2}\sum_{\nu}b_{j\nu}e^{-i(N-\nu)\vartheta} \ .$$

Then, from Eq. (1.5), it follows that

$$|\Psi_{\tilde{E}}(\mathbf{r},\mathbf{R})\rangle=-\frac{2\pi}{m}\sum_{j=1}^{2}G_L(\tilde{E};\mathbf{r},\mathbf{R}_j)|B_j\rangle \ . \quad (2.3)$$

Applying the boundary conditions (2.2) to $\psi_{\tilde{E}}(\mathbf{r},\mathbf{R})$, and assuming an elliptically polarized laser field in the dipole approximation, two infinite systems of coupled linear equations for the coefficients $b_{j\mu}$, $j=1,2$, $\mu=0,\pm1,\pm2,\ldots$ are obtained

$$\kappa_1 b_{1\mu}+\sum_{\nu}F_{\mu\nu}(\tilde{E})b_{1\nu}+\sum_{\nu}S_{\mu\nu}(\tilde{E};\mathbf{R}_1,\mathbf{R}_2)b_{2\nu}=0 \ , \quad (2.4a)$$

$$\sum_{\nu}S_{\mu\nu}(\tilde{E};\mathbf{R}_2,\mathbf{R}_1)b_{1\nu}+\kappa_2 b_{2\mu}+\sum_{\nu}F_{\mu\nu}(\tilde{E})b_{2\nu}=0 \ , \quad (2.4b)$$

where

$$F_{\mu\nu}(\tilde{E})=\frac{1}{2\pi}\int_0^{2\pi}d\vartheta\, e^{-i(N-\mu)\vartheta}\times\frac{1}{2\pi}\int_0^{2\pi}d\vartheta'\,F(\tilde{E};\vartheta,\vartheta')e^{i(N-\nu)\vartheta'} \quad (2.5a)$$

with

$$F(\tilde{E};\vartheta,\vartheta')=\frac{e^{i\Phi(\vartheta,\vartheta')}}{f(\vartheta,\vartheta')}\times\sum_{\nu}e^{i(N-\nu)(\vartheta-\vartheta')}[e^{ik_\nu(\tilde{E})f(\vartheta,\vartheta')}-1] \quad (2.5b)$$

and

$$S_{\mu\nu}(\tilde{E};\mathbf{R}_1,\mathbf{R}_2)=-\frac{2\pi}{m}\int_0^{2\pi}\frac{1}{2\pi}d\vartheta\int_0^{2\pi}d\vartheta'e^{-i(N-\mu)\vartheta}G_L(\tilde{E};\mathbf{R}_1,\vartheta;\mathbf{R}_2,\vartheta')e^{i(N-\nu)\vartheta'} \ . \quad (2.6)$$

$G_L$ is given by (A10) and (A11) of Appendix A. For a circularly polarized laser field this yields

$$S_{\mu\nu,\mathrm{cir}}(\tilde{E};\mathbf{R}_1,\mathbf{R}_2)=\frac{1}{2\pi}\int_0^{2\pi}d\vartheta\,e^{i\mu\vartheta}\frac{1}{2\pi}\int_0^{2\pi}d\vartheta'\,e^{-i\nu\vartheta'}\sum_{\nu'}e^{-i\nu'(\vartheta-\vartheta')}\frac{\exp\{i[k_{\nu'}(\tilde{E})|\mathbf{R}_1-\mathbf{R}_2-\mathbf{f}(\mathbf{R}_1,\vartheta;\mathbf{R}_2,\vartheta')|]\}}{|\mathbf{R}_1-\mathbf{R}_2-\mathbf{f}(\mathbf{R}_1,\vartheta;\mathbf{R}_2,\vartheta')|} \ , \quad (2.7a)$$

where

$$|\mathbf{R}_1-\mathbf{R}_2-\mathbf{f}(\mathbf{R}_1,\vartheta;\mathbf{R}_2,\vartheta')|=h(\vartheta-\vartheta',\mathbf{R})(1-g)^{1/2} \ , \quad (2.7b)$$

$$h(x,\mathbf{R})=\left[R^2+2\alpha_0^2\sin^2\left[\frac{x+\mathbf{k}\cdot\mathbf{R}}{2}\right]\right]^{1/2} \ , \quad (2.7c)$$

$$g=\frac{2^{5/2}\alpha_0\sin(\varphi_-)\mathbf{R}\cdot\hat{\mathbf{n}}(\varphi_+)}{R^2+2\alpha_0^2\sin^2(\varphi_-)} \ , \quad (2.7d)$$

and

$$\hat{\mathbf{n}}(\varphi)=\hat{\mathbf{e}}_1\cos(\varphi)+\hat{\mathbf{e}}_2\sin(\varphi) \ ,$$
$$2\varphi_\pm=\vartheta\pm\vartheta'-\mathbf{k}\cdot(\mathbf{R}_1\pm\mathbf{R}_2) \ . \quad (2.7e)$$

In order to diagonalize the system of equations (2.4), one needs an additional approximation: $g\ll 1$. Note that $g=0$ if $\hat{\mathbf{R}}\|\hat{\mathbf{k}}$. The approximation is better (i.e., it includes a broader region of angles between $\hat{\mathbf{k}}$ and $\hat{\mathbf{R}}$) if the interpotential distance is larger (or if the field is stronger). The details of the approximation are discussed in Appendix C. Then the equation for eigenenergies is obtained in the form

$$[\kappa_1+F(\tilde{\varepsilon})][\kappa_2+F(\tilde{\varepsilon})]=S(\tilde{\varepsilon},\mathbf{R})S(\tilde{\varepsilon},-\mathbf{R}) \ , \quad (2.8a)$$

where

$$F(\tilde{\varepsilon})=\int_0^{2\pi}\frac{1}{2\pi f(x)}dx\sum_{\nu}e^{-i\nu x}[e^{ik_\nu(\tilde{\varepsilon})f(x)}-1] \ , \quad (2.8b)$$

$$S(\tilde{\varepsilon},R)=\int_0^{2\pi}\frac{1}{2\pi h(x,\mathbf{R})}dx\sum_{\nu}e^{-i\nu x+ik_\nu(\tilde{\varepsilon})h(x,\mathbf{R})} \ , \quad (2.8c)$$

and

$$f(x)=2^{1/2}\alpha_0|\sin(x/2)| ,$$
$$k_\nu^2=2m(\tilde{\varepsilon}-U_p+\nu\omega) , \tag{2.8d}$$
$$\tilde{\varepsilon}=\varepsilon_j+\Delta-i/2\Gamma, \quad j=1 \text{ or } 2 .$$

Using the coordinate-phase representation and within the approximation $g\ll 1$, another form of the eigenvalue equation can be derived which we present here without any further details of its derivation:

$$[\kappa_1'(\tilde{\varepsilon})+G(\tilde{\varepsilon})][\kappa_2'+G(\tilde{\varepsilon})]=S(\tilde{\varepsilon},\mathbf{R})S(\tilde{\varepsilon},-\mathbf{R}) , \tag{2.9a}$$

where

$$G(\tilde{\varepsilon})=\left[\frac{m\omega}{2\pi i}\right]^{1/2}\int_0^\infty dx\, x^{-3/2}e^{i\tilde{\varepsilon}x} \times\left[\exp\left[i\frac{m\omega}{2x}f^2(x)\right]-1\right] , \tag{2.9b}$$

$$\kappa'(\tilde{\varepsilon})=\kappa-[-2m(\tilde{\varepsilon}-U_p)]^{1/2} , \tag{2.9c}$$

$$\omega\tilde{\epsilon}=\tilde{\varepsilon}-U_p , \tag{2.9d}$$

and

$$S(\tilde{\varepsilon},\mathbf{R})=\left[\frac{m\omega}{2\pi i}\right]^{1/2}\int_0^\infty dx\, x^{-3/2} \times\exp\left[i\tilde{\varepsilon}x+i\frac{m\omega}{2x}h^2(x,\mathbf{R})\right] . \tag{2.9e}$$

Introducing the notation

$$w_j=\omega/|\varepsilon_{0j}|, \quad \varepsilon_{0j}=-\frac{\kappa_j^2}{2m}, \quad j=1,2 , \tag{2.10a}$$
$$f(x,\mathbf{R})=\left[1+a\sin^2\left[\frac{x}{2}-b\right]\right]^{1/2} , \tag{2.10b}$$
$$a=2\left[\frac{\alpha_0}{R}\right]^2=2\frac{I}{I_A}\left[\frac{2\mathcal{R}}{\omega}\right]^4\left[\frac{a_B}{R}\right]^2 , \tag{2.10c}$$
$$b=\hat{\mathbf{k}}\cdot\hat{\mathbf{R}}\frac{\omega R}{2}=\frac{R}{a_B}\frac{\omega}{\mathcal{R}}\frac{\alpha_F}{4}\hat{\mathbf{k}}\cdot\hat{\mathbf{R}} ,$$
$$k_\nu(\tilde{\varepsilon})R=\left[\frac{\omega}{\mathcal{R}}\right]^{1/2}\frac{R}{a_B}\left[\nu+\frac{\tilde{\varepsilon}-U_p}{\omega}\right]^{1/2} , \tag{2.10d}$$
$$p_\omega=\frac{R}{a_B}\left[\frac{\omega}{\mathcal{R}}\right]^{1/2} , \tag{2.10e}$$

where $I_A=3.5\times10^{16}$ W/cm$^2$ is the atomic unit of the laser-field intensity and $\mathcal{R}$ is the Rydberg energy. Equation (2.8a) transforms into

$$[w_1^{-1/2}-z-I(z^2,B)][w_1^{-1/2}-z-I(z^2,B)] =J(\tilde{\varepsilon},\mathbf{R})J(\tilde{\varepsilon},-\mathbf{R}) , \tag{2.11}$$

where

$$U_p=\frac{\omega}{4}B, \quad B=\left[\frac{2\mathcal{R}}{\omega}\right]^3\frac{I}{I_A} , \tag{2.12a}$$
$$z_j^2=\frac{U_p-\varepsilon_j}{\omega}-X_1^{(j)}+iX_2^{(j)} ,$$
$$X_1^{(j)}=\frac{\Delta_j}{\omega} , \tag{2.12b}$$
$$X_2^{(j)}=\frac{\Gamma_j}{2\omega} ,$$

and

$$I(z^2,B)=(4\pi i)^{-1/2}\int_0^\infty dx\, x^{-3/2}e^{-iz^2x}\left[1-\exp\left[\frac{i}{x}B\sin^2(x/2)\right]\right] , \tag{2.13a}$$
$$J(\tilde{\varepsilon},\mathbf{R})=\frac{1}{p_\omega}\int_0^{2\pi}\frac{1}{2\pi f(x,\mathbf{R})}dx\sum_\nu\exp[-i\nu x+ik_\nu(\tilde{\varepsilon})Rf(x,\mathbf{R})]$$
$$=(4\pi i)^{-1/2}\int_0^\infty dx\, x^{-3/2}\exp\left[-iz^2x+\frac{i}{x}\frac{B}{a}f^2(x,\mathbf{R})\right] . \tag{2.13b}$$

Boundary conditions, applied to the asymptotics of the electron wave function with the complex quasienergy, discussed in Sec. III [Eq. (3.2)], yield the choice of a proper sheet of the Riemann surface. Then, Eq. (2.11) has only two physical solutions

$$\tilde{\varepsilon}_j=\varepsilon_j+\Delta_j-\frac{i}{2}\Gamma_j, \quad j=1,2 , \tag{2.14}$$

where $\varepsilon_j$ in the eigenenergy in absence of the laser field.

The right-hand side of Eq. (2.13a) can be expanded in series of powers of $B$:

$$I(z^2,B)=\sum_{\mu=-\infty}^{\infty}I_\mu(z^2,B) , \tag{2.15a}$$

where

$$I_\mu(z^2,B)=(-1)^\mu(z^2-\mu)^{1/2} \times\sum_{n=\max(1,|\mu|)}^{\infty}\frac{[B(z^2-\mu)]^n}{(2n+1)(n-\mu)!(n+\mu)!} , \tag{2.15b}$$

while the integral $J(\tilde{\varepsilon},\mathbf{R})=J(z^2,a,p_\omega b)$ is expanded as

$$p_\omega J(z^2,a,p_\omega,b)=\exp(-p_\omega z) + \sum_{n=1}^{\infty}(-1)^n(2n-1)!!2^{-2n}a^n \times S_n(z^2,p_\omega,b)\ , \tag{2.16a}$$

where

$$S_n(z^2,p_\omega,b) = \sum_{m=-n}^{n}\frac{(-1)^n e^{i2mb}}{(n-m)!(n+m)!}\mathcal{K}_n(p_\omega(z^2+m)^{1/2}) \tag{2.16b}$$

with

$$\mathcal{K}_n(z)=\left[\frac{2}{\pi}\right]^{1/2} z^{n+1/2}K_{n+1/2}(z) \tag{2.16c}$$

and $K_\nu(z)$ are McDonald's functions [16]. Note that $\mathcal{K}_n(z)$ can be calculated using the recurrence relations

$$\mathcal{K}_{n+1}(z)=z^2\mathcal{K}_{n-1}(z)+(2n+1)\mathcal{K}_n(z)\ , \quad n=0,1,2,\ldots \tag{2.17a}$$

and the properties

$$z\mathcal{K}_{-1}(z)=\mathcal{K}_0(z)=e^{-z}\ ,$$
$$\lim_{z\to 0}\mathcal{K}_n(z)=1\ , \tag{2.17b}$$
$$\lim_{z\to\infty}\mathcal{K}_n(z)=0\ .$$

The expansions (2.15) and (2.16) are used to solve Eq. (2.11) numerically and these need to be discussed in detail. According to (2.17), $J(\tilde{\varepsilon},\mathbf{R})\to 0$ as $R\to\infty$, i.e., the two ZRP's become independent, and Eq. (2.11) splits into two independent equations which define eigenenergies for the electron which move in the vicinity of one ZRP. One of these is

$$w_1^{-1/2}-z-I(z^2,B)=0\ , \tag{2.18}$$

which can be shown to agree with the eigenvalue equation derived by Manakov [1] and Berson [2]. Since $g\to 0$ for $R\to\infty$, there is no longer any condition to be satisfied, and Eq. (2.18) is exact. The $\mu$th term in the sum for $I(z^2,B)$, Eq. (2.15a), corresponds to the $\mu$-photon ionization ($\mu\geq\mu_0$). The sum in Eq. (2.15b) runs over the powers of the laser intensity [contains $B^n\simeq(I/I_A)^n$, $n\geq|\mu|$]. By standard methods [17], it can be shown that the series in $n$ converges absolutely for all $B$ and $\omega$, within the intervals of $I$ defined by the zeros of $z^2-\mu$. The points of nonanalyticity of the functions $(z^2-\mu)^{n+1/2}$, i.e., the branching points of $I(z^2,B)$, are at $z^2-\mu=0$. The channel for a $\mu$-photon ionization closes when the intensity $I$ reaches some limiting value, defined by $\mathrm{Re}(z^2-\mu)=0$. The closing happens due to an increase of the ionization potential $|\varepsilon_0-U_p+\Delta|$. From the general theory [13] it follows that the total width $\Gamma$ can be written as a sum of partial widths $\Gamma_\mu$. At low laser intensities, all $\mu\geq\mu_0$ photon processes contribute to the width $\Gamma$, i.e., $\Gamma=\sum_{\mu\geq\mu_0}\Gamma_\mu$. When $I$ increases, $\mathrm{Re}(z^2\omega)$ increases too. This induces closing of all channels $\mu_0\leq\mu\leq\mu_1$, and therefore $\Gamma=\sum_{\mu>\mu_1}\Gamma_\mu$. On the other hand, the integral $J(\tilde{\varepsilon},\mathbf{R})$ is expanded in a series over the parameter $a=B/(p_\omega/2)^2$. Therefore, the expansion for $I(z^2,B)$ and $J(\tilde{\varepsilon},\mathbf{R})$ are both expansions in the field intensity. By the change of the order of summation in (2.16), it follows that the $\mu$th term in series (2.16) corresponds to the $\mu$th photon process, and the sum over $n$ is absolutely convergent. The branching points are again those where $(z^2-\mu)^{1/2}=0$. Note that, with the two ZRP's at distance $R<R_g$, the eigenenergy $\varepsilon_1$ is complex, $\varepsilon_1=\mathrm{Re}\varepsilon_1-i\Gamma_R/2$, even if the laser field is not present. One can write

$$\varepsilon_\mu=\varepsilon-U_p+\Delta+\mu\omega\ , \tag{2.19a}$$
$$q_\mu=[2m(\varepsilon_\mu-i\Gamma/2)]^{1/2}\ , \tag{2.19b}$$
$$\Gamma\ll\varepsilon_{\mu_0}<\omega\ . \tag{2.19c}$$

If $R>R_g$, or if the ionization originates from the ground term $\varepsilon_2$, $\varepsilon$ in Eq. (2.19a) stands for $\varepsilon_1$ or $\varepsilon_2$, while $\Gamma$ in Eqs. (2.19b) and (2.19c) should be replaced by $\Gamma_1$ or $\Gamma_2$, with $\mu_0>0$, $\varepsilon_\mu>0$, and $\Delta\to\Delta_1$ or $\Delta_2$. But, when $R<R_g$, $\varepsilon_1$ becomes complex and the relation (2.19) applies with $\varepsilon\to\mathrm{Re}\varepsilon_1$, $\Gamma\to\Gamma_R+\Gamma_1$, and $\Delta\to\Delta_1$, with $\mu_0<0$. Since $\mathrm{Re}\varepsilon_1>0$, the absorption of photons from the field is not a necessary condition for ionization. Furthermore, it can be that $\mu<0$, i.e., photons are emitted during the process of ionization. The total ionization rate $\Gamma_R+\Gamma_1$ is then smaller (Sec. III) than the ionization rate in the absence of the laser field $\Gamma_R$. We note that contributions to $\Gamma_1$ comes from all partial $\Gamma_{1\mu}$ with $\mu\geq\mu_0$, where $\mu_0<0$, i.e., $\Gamma_1=\sum_{\mu\geq\mu_0}\Gamma_{1\mu}$.

## III. DISCUSSION OF THE RESULTS

Equation (2.11) is solved numerically for complex eigenenergies of an electron in presence of both ZRP's and a circularly polarized laser field. To compare our results with possible experiments, the parameters were also chosen to model the $H_2^-$ (symmetric) and $OH^-$ (asymmetric) ions. In the case of the atomic ion $H^-$, the quasienergy of which is obtained as a special case of our procedure, Eq. (2.18), the range of the laser field parameters is extended in comparison with the previous calculations [1-5,18].

### A. Atomic case

Equation (2.18) was solved using the expansion (2.15). The key parameters upon which the results depend are the laser field intensity, the frequency, and the ionization potential of the model atom (ion). Figure 2 shows $\Delta/\omega$ and $\Gamma/2\omega$ as functions of parameter $B$, for different values of $w$, $w=0.5$, 1, 2, 5, and 10. Jumps on the curves correspond to the branching points of the function $(z^2-\mu)^{1/2}$. According to Fig. 2(b), the width increases nearly linearly with the laser-field intensity if $w>1$. When $U_p-\Delta$ becomes large enough, the ionization may

occur only by a two-photon ionization. As a consequence, after passing through the region of a local minimum, the curve changes its slope. This is connected with the fact that when the intensity (i.e., parameter $B$) is such that the $\mu$-photon ionization channel is closed, the resonance and shadow poles interchanges roles [18,19] (this will be explained in detail later). The linear dependence of $\Delta$ and $\Gamma$ on $B$ (if $B \ll 1$ and $w > 1$) can be derived analytically. The term $\mu = 1$ in expansion (2.15) corresponds to the one-photon ionization. If $B \ll 1$, the first term of the expansion is dominant, and therefore the approximate solution of Eq. (2.18) may be written as [1,2]

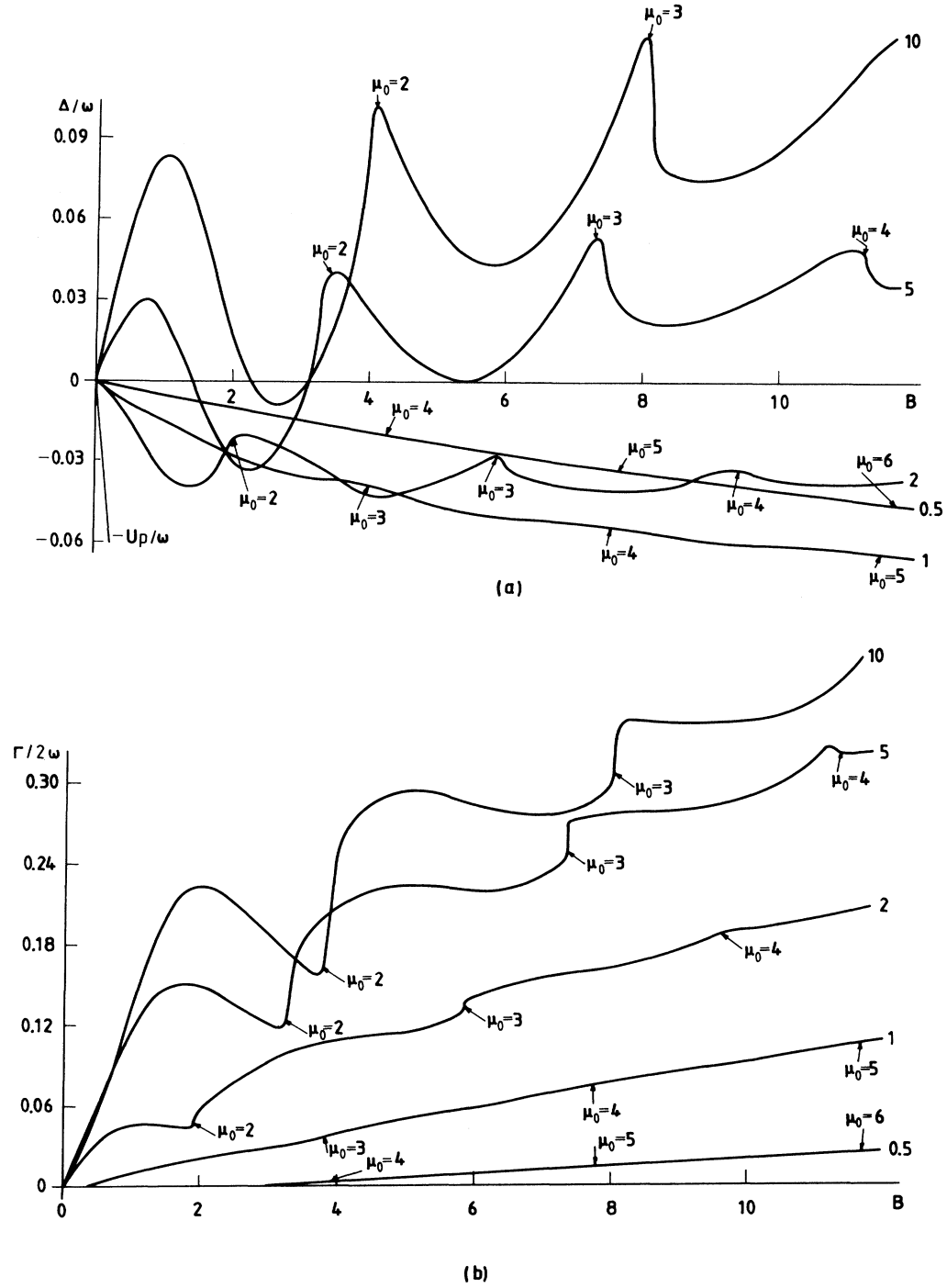


FIG. 2. (a) Shift $\Delta$ and (b) width $\Gamma$ of the bound-state energy $\varepsilon_0$ of an electron in one ZRP vs the laser-field intensity parameter $B$ for different values of the parameter $w = \omega/|\varepsilon_0| = 0.5$, 1, 2, 5 and 10. $\mu_0$ is the minimum number of photons to ionize.

$$\left[\Delta-\frac{i}{2}\Gamma\right]\Big|_{B\ll 1} = \frac{\omega B}{4}\{1-4/(3w^2)[(1+w)^{3/2}-2+i(w-1)^{3/2}]\} . \tag{3.1}$$

From Fig. 2 it is obvious that the maxima and positions of the branching points are shifted toward larger $B$'s and are more pronounced if $w$ is larger. The reason is that $z^2$ becomes smaller with the increase of $w$ ($U_p$ is smaller, i.e., the ionization potential is smaller). Then larger values of $B$ are needed to close the $\mu$-photon ionization channel. The shift of the ionization potential is $\Delta-U_p$. It is important to note that, if the laser field is strong enough, the principal contribution to this shift comes from the ponderomotive potential, which exceeds the laser-induced ac Stark shift by many orders of magnitude.

The choice of the sign of the square root $(z^2-\mu)^{1/2}$ in calculations deserves some attention. The complex momentum of the electron incurred by ionization is

$$\begin{aligned} q_\mu &= [2m(\varepsilon_\mu - i\Gamma/2)]^{1/2} \\ &= [2m(\varepsilon_0 - U_p + \Delta + \mu\omega - i\Gamma/2)]^{1/2} \\ &= [-2m(z^2-\mu)\omega]^{1/2} . \end{aligned}$$

The asymptotic limit of the electron wave function as $r\to\infty$ is of the form $\exp(iq_\mu r)/r$. Since this limit has to give a divergent wave, and since $\varepsilon_\mu>0$ and $\mathrm{Re}q_\mu>0$, it follows that

$$\text{if } \mathrm{Re}(z^2-\mu)<0 \text{ then } \mathrm{Re}(\mu-z^2)^{1/2}>0 . \tag{3.2a}$$

It should be mentioned that, since $\Gamma>0$, we have $\mathrm{Im}q_\mu<0$ if $\mathrm{Re}q_\mu>0$, which is the usual condition for resonances [18,19].

Similarly, when the ionization channel is closed ($\varepsilon_\mu<0$), the eigenfunction has to decrease exponentially with $r$ as $\exp(-q_\mu r)$, i.e.,

$$\text{if } \mathrm{Re}(z^2-\mu)>0 \text{ then } \mathrm{Im}(\mu-z^2)^{1/2}>0 . \tag{3.2b}$$

The choice of the sign of the square root is uniquely determined by the conditions (3.2a) and (3.2b). Condition (3.2a) is equivalent to $\mathrm{Im}(z^2-\mu)^{1/2}<0$, while (3.2b) gives $\mathrm{Re}(z^2-\mu)^{1/2}>0$.

Other combinations of parameters may be also used in presenting $\Gamma$ and $\Delta$. One of these, originally introduced by Berson [2], is defined as $V=2|\mathcal{R}/\varepsilon_0|^{3/2}(I/I_A)^{1/2}$, and therefore $B=2V^2/w^3$. $\Delta/|\varepsilon_0|$ and $\Gamma/|2\varepsilon_0|$ versus $V$, for $w=2$, 5, and 10 are given in Fig. 3. Our numerical results agree with the Berson's in the range of parameter $V$ which was considered by him ($V<1.5$ for $\Delta$ and $V<1$ for $\Gamma$). Furthermore, we are able to compute $\Delta$ and $\Gamma$ for a much greater value of $V$ ($V\simeq 50$ in Fig. 3). The branching points are defined by

$$V_\mu = 2^{1/2}w(\mu w - 1 + \Delta/|\varepsilon_0|)^{1/2} ,$$

and the difference between two successive $V_\mu$ can be used to define a local period of oscillations. For example, if $w=5$ then $\Delta V_{21}=V_2-V_1\cong 7$. It is important to note that, if $V$ is larger than 15, $\Gamma/2|\varepsilon_0|$ approaches 1 and therefore $\Gamma$ loses its meaning of the ionization rate.

Potvliege and Shakeshaft (Sec. III of Ref. [18]) have also studied a short-range potential simulating a negative atomic ion. Their Fig. 8 shows a similar behavior of $\Gamma$. They follow the path (in the complex $\tilde{\varepsilon}$ plane versus laser-field intensity $I<8\times10^{13}$ W/cm$^2$) of a resonance pole (of the scattering amplitude) which starts as a bound state ($\varepsilon_0\cong-1.09$ eV), in the presence of a linearly polarized laser field of frequency $\omega=2.33$ eV. The resonance pole is a dominant one if the laser-field intensity is below the threshold (after which the channel for one-photon ionization is closed). If the intensity increases further, the resonance pole interchanges its role with a nearby shadow pole (which lie on some of the additional unphysical sheets of the Riemann surface, see Ref. [18] and references therein). To compare our results with theirs, in Figs. 4 and 5 we present the results for the $H^-$ system ($\varepsilon_0=-0.7542$ eV). In the Fig. 4 the width $\Gamma$ is presented versus the laser-field intensity $I<2.5\times10^{14}$ W/cm$^2$ and photon frequency $\omega=2$ eV. $\mu_0$ is the minimum number of photons needed to ionize. The results presented in Fig. 4 are qualitatively similar to the results of Ref. [18]. The width $\Gamma$ increases from zero when $I$ increases, passes through a local maximum for some $I$, and decreases.

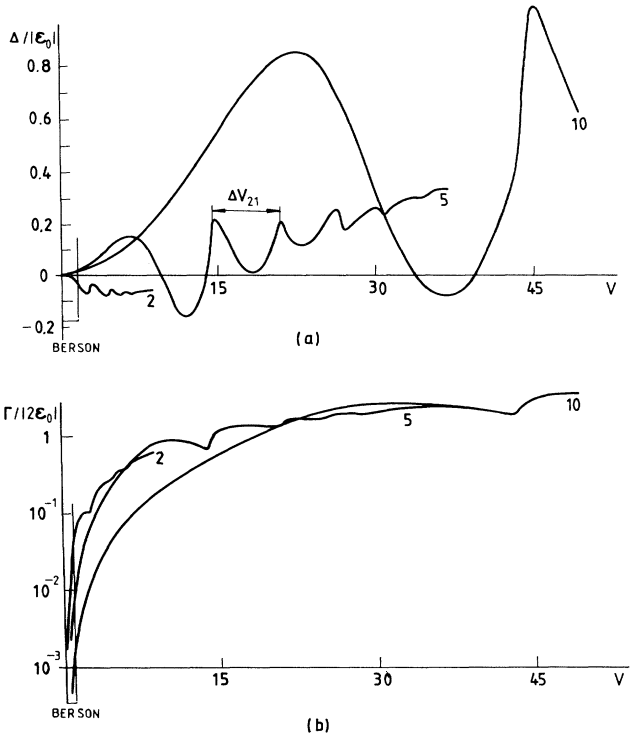


FIG. 3. (a) Shift $\Delta$ and (b) width $\Gamma$ of the bound-state energy $\varepsilon_0$ of an electron in one ZRP vs $V=2|\mathcal{R}/\varepsilon_0|^{3/2}(I/I_A)^{1/2}$, for different values of the parameter $w=2$, 5, and 10. The interval of $V<1.5$ was considered by Berson [2]. $\Delta V_{21}=V_2-V_1$ is a distance between successive branching points of the function $[z^2(V)-\mu]^{1/2}$, $\mu=1.2$.

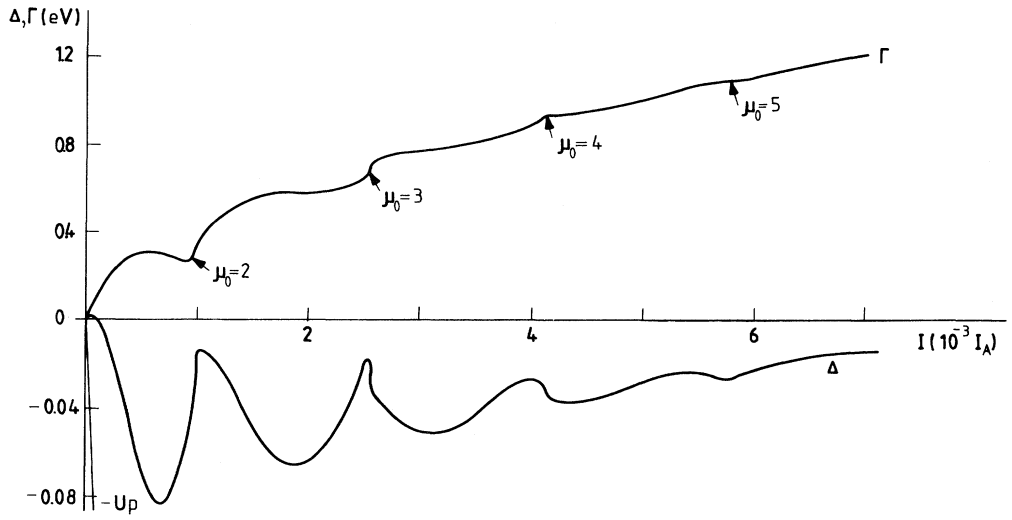


FIG. 4. Shift $\Delta$ and width $\Gamma$ of the ground state of $H^-$, calculated in the model of one ZRP, vs the laser-field intensity $I$, with the photon frequency of $\omega=2$ eV. $U_p$ is the ponderomotive potential. $\mu_0$ is the minimum number of photons needed to ionize.

After the first threshold ($\mu_0=2$), the conditions (3.2) are fulfilled for the $(\mu-z^2)^{1/2}$ which correspond to a different sheet of the Riemann surface, the shadow pole becomes dominant and $\Gamma$ increases again with increasing intensity $I$. In Fig. 4 there are four thresholds presented at which resonance and shadow poles interchange their roles.

If the frequency is low enough (Fig. 4), even for $I \ll I_A$, the width takes values of order of 1 eV and, therefore, the condition $\Gamma \ll \varepsilon_{\mu_0}=\varepsilon_0-U_p+\Delta+\mu_0\omega<\omega$ is violated. On the other hand, the condition above is also not fulfilled in the vicinity of branching points of $(z^2-\mu)^{1/2}$ since $z^2-\mu=0$ yields $\varepsilon_\mu=0$. In fact, the channel $\mu$ closes and the energy of outgoing electron becomes vanishingly small. A further increase of $I$ opens a new channel $\mu$ where $\Gamma \ll \varepsilon_\mu$. For example, in the case of the $H^-$ ion, with $\omega=2$ eV and $I=9.3\times10^{-4}I_A$ it follows that $\mu_0=1$, $\varepsilon_1=0.026$ eV, and $\Gamma=0.279$ eV. But $I=9.7\times10^{-4}I_A$ yields $\mu_0=2$, $\varepsilon_2=2$ eV, and $\Gamma=0.32$ eV.

The values on the abscissa of Fig. 4 can be related to other parameters of interest: $I=x\times10^{-3}I_A$, $B=2.52x$,

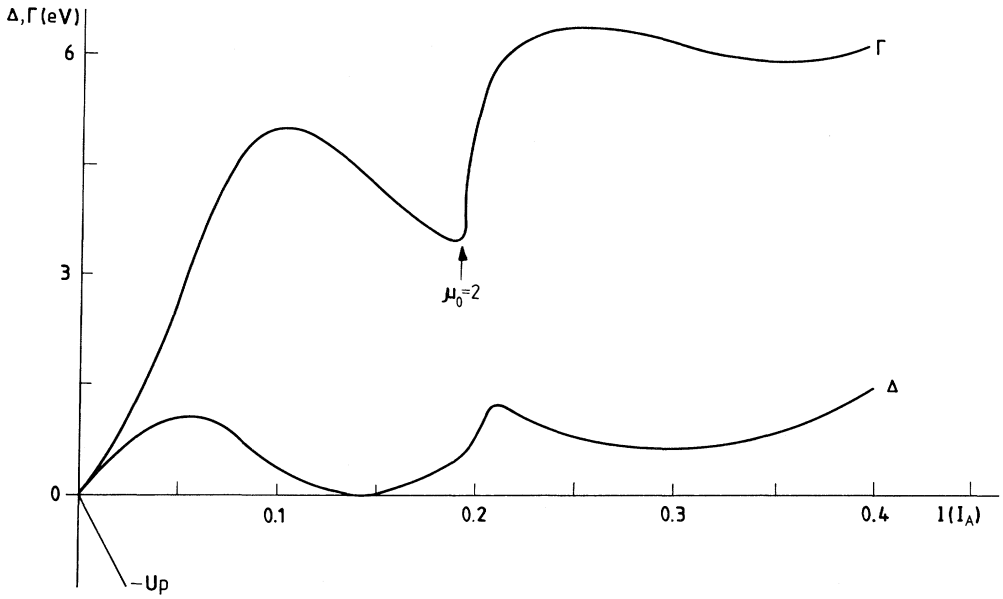


FIG. 5. Shift $\Delta$ and width $\Gamma$ of the ground state of $H^-$ ion vs the laser field intensity $I$ at the photon frequency of $\omega=10$ eV. $\mu_0$ is the minimum number of photons needed to ionize.

$U_p = 1.26x$ eV, $\alpha_0 = 5.85x^{1/2} a_B$ and $V = 4.84x^{1/2}$. Similarly, in Fig. 5, one has $I = xI_A$, $B = 20x$, $U_p = 50x$ eV, $\alpha_0 = 7.4x^{1/2} a_B$, and $V = 153x^{1/2}$. Therefore, the parameter $\alpha_0$ reaches values of $16a_B$ in Fig. 4, but the frequency is not sufficiently high ($\omega = 2$ eV) to make a comparison with the standard high-frequency approximation [20]. On the other hand, in Fig. 5, the frequency is high enough ($\omega = 10$ eV) but the parameter $\alpha_0$ reaches values of $4.7a_B$, which is too low to be in the atomic dichotomy regime [21]. Therefore, our results do not contradict to the results of high-frequency–high-intensity approximation of Gavrila [21] where the width of a bound state decreases as a result of atomic dichotomy, in the limit $\alpha_0 \gg 1$.

### B. Molecular case

Before we discuss the physical content of our numerical results, it is useful to derive an approximate solution of Eq. (2.11), in the limit $I \ll I_A$. The parameter $z$, Eq. (2.12b), can be written in the form

$$z = z_0 + \Delta z, \quad z_0^2 = -\frac{\varepsilon}{\omega} = x_0 + iy_0 = r_0 e^{i\varphi_0} , \tag{3.3}$$

where $z_0$ is a solution of the eigenvalue equation (1.15) in absence of the laser field. Equation (1.15) is rewritten in the form

$$(p_1 - p_r)(p_2 - p_r) = e^{-2p_r} , \tag{3.4a}$$

where

$$p_r = p_\omega z_0 = \frac{R}{a_B}\left[-\frac{\varepsilon}{\mathcal{R}}\right]^{1/2} ,$$
$$p_j = \frac{R}{a_B}\left|\frac{\varepsilon_{0j}}{\mathcal{R}}\right|^{1/2} , \quad j = 1,2 . \tag{3.4b}$$

Of the two complex conjugate solutions of (3.4), the one with $\mathrm{Im}(z_0^2) = \Gamma_R/(2\omega) > 0$ is chosen. If, the terms of order $(I/I_A)^2$ are neglected in Eq. (2.11) [i.e., the terms of the order $B^l a^m (\Delta z/z_0)^n$, $l + m + n \geq 2$] and the relation (3.4) is used, it follows that

$$\Delta z = (\alpha - \beta)/\gamma , \tag{3.5a}$$

$$\alpha = \frac{B}{3}(p_1 + p_2 - 2p_r) Y_1(z_0^2) , \tag{3.5b}$$

$$Y_1(z) = z^{3/2} - \tfrac{1}{2}[(z+1)^{3/2} + (z-1)^{3/2}] , \tag{3.5c}$$

$$\beta = \frac{a}{4p_\omega}\exp(-p_r) \sum_{\nu=\pm 1} S_1(z_0^2, p_\omega, \nu b) , \tag{3.5d}$$

$$\gamma = 2\exp(-2p_r) + 2p_r - p_1 - p_2 . \tag{3.5e}$$

The obtained result for $\Delta z$ is linear in the field intensity. When $\varepsilon$ is real, the solution simplifies since

$$Y_1(z_0^2) = z_0^3 - \tfrac{1}{2}(1+z_0^2)^{3/2} - \frac{i}{2}(1-z_0^2)^{3/2} , \tag{3.6a}$$

$$\beta = \frac{a}{2p_\omega}\exp(-p_r)[(1+p_r)\exp(-p_r) - \tfrac{1}{2}\cos(2b) F(z_0^2)] , \tag{3.6b}$$

$$F(z_0^2) = e^{ip} - (1 - ip_-) + \exp(-p_+)(1+p_+) , \tag{3.6c}$$
$$p_\pm = p_\omega (1 \pm z_0^2)^{1/2} .$$

Note that $\Delta$ and $\Gamma$ are given in terms of $\Delta z$ as

$$\Delta = \omega X_1 = U_p - \omega\,\mathrm{Re}[\Delta z(2z_0 + \Delta z)] ,$$
$$\Gamma = 2\omega X_2 = 2\omega\,\mathrm{Im}[\Delta z(2z_0 + \Delta z)] . \tag{3.7}$$

Obviously, the width is not vanishingly small only if $z_0^2 < 1$, i.e., $|\varepsilon| < \omega$. The applicability of the derived approximation depends upon parameters $B$ and $a$, where

$$B = v^{-3}\frac{I}{I_A}, \quad a = 2v^{-4} r^{-2}\frac{I}{I_A}, \quad v = \frac{\omega}{2\mathcal{R}}, \quad r = \frac{R}{a_B} . \tag{3.8}$$

It should be noted that the parameters $B$ and $a$ are inversely proportional to the third and fourth power of the field frequency, respectively. To have convergence of the obtained expansions for $I \ll I_A$, the frequency should not be too low in comparison with $\mathcal{R}$. Since $a$ is inversely proportional to the square of the internuclear distance, $R$ is supposed to be not too small in comparison with $a_B$. For $R \gg a_B$, the $\varepsilon$ is real, and one obtains

$$\Delta z|_{R \gg a_B} = -\frac{B}{3} Y_1(z_0^2) ,$$
$$X_2|_{R \gg a_B} = \frac{B}{3} z_0 (1 - z_0^2)^{3/2} , \tag{3.9}$$

which is in agreement with the approximate solution for one ZRP, Eq. (3.1).

The above analysis can be used to discuss the dependence of $\Delta$ and $\Gamma$ on $R$, when $I \ll I_A$. The approximate results for the $H_2^-$ ion, at $\omega = 3$ eV, are presented in Fig. 6. These solutions coincide with the exact numerical solutions if $I < 10^{12}$ W/cm$^2$. The limiting values $\Delta_g$ and $\Gamma_g$ are

$$\Delta_{jg} = \lim_{R \to \infty} \Delta_j \tag{3.10a}$$
$$= U_p\{1 + \tfrac{4}{3} e_j^{1/2}[2e_j^{3/2} - (1+e_j)^{3/2}]\} , \tag{3.10a}$$
$$\Gamma_{jg} = \lim_{R \to \infty} \Gamma_j = \tfrac{8}{3} U_p e_j^{1/2}(1 - e_j)^{3/2} ,$$
$$e_j = \left|\frac{\varepsilon_{0j}}{\omega}\right|, \quad j = 1,2 . \tag{3.10b}$$

In this example $e_1 = e_2$ and

$$\Delta_g = 130\frac{I}{I_A}\ \text{eV}, \quad \Gamma_g = 484\frac{I}{I_A}\ \text{eV} . \tag{3.10c}$$

Note that here $\Delta$ is of the same order of magnitude as $U_p$, which is not true at higher laser intensities.

Since $\varepsilon_2(R)$ is always real and negative, $\Delta_2(R)$ and $\Gamma_2(R)$ behave regularly, without sudden jumps (this is not true for higher laser intensities where branching points

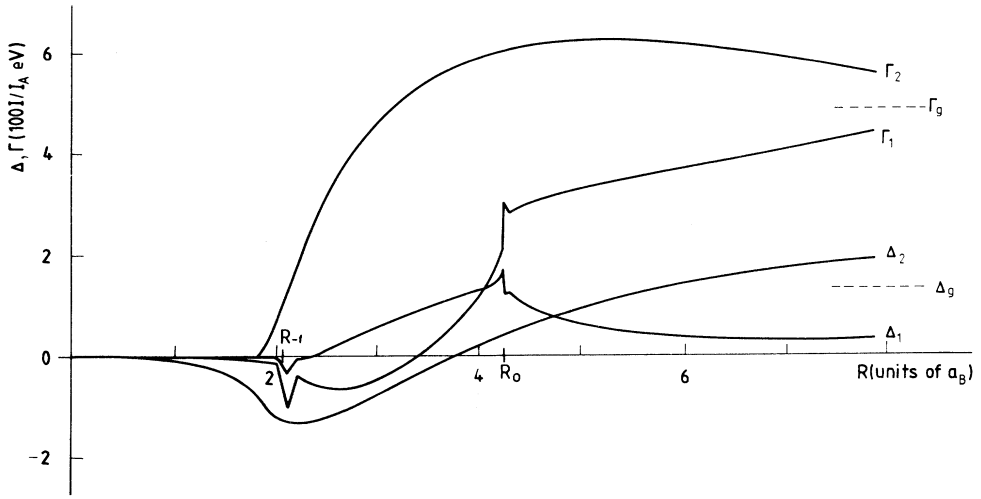


FIG. 6. Scaled shifts ($\Delta$) and widths ($\Gamma$) of the electronic terms of the $H_2^+$ ion vs internuclear distance $R$, at $\omega=3$ eV and in approximation $I \ll I_A$. $\Delta$ and $\Gamma$ coincide with the exact results if $I < 10^{12}$ W/cm$^2$. $\Delta_g$ and $\Gamma_g$ are the limiting values when $R \to \infty$. Indices 1 and 2 stand for the higher and lower terms of Fig. 1, respectively.

appear). The shift $\Delta_2$ starts from vanishingly small values, decreases to negative values as $R$ increases, and has a minimum $\Delta_2(R=2.2a_B)=-132I/I_A$ eV. After that it increases to $\Delta_g$. This means that the effect of the laser field is to increase the depth of the potential well of a molecular electronic state. The width $\Gamma_2$ is significant only if $|\varepsilon_2| < \omega = 3$ eV, i.e., if $R > 1.8a_B$. It increases with $R$, passes through a maximum

$$\Gamma_{2,\max}=\Gamma_2(R=5.2a_B)=621I/I_A \text{ eV}$$

and tends to $\Gamma_g$ as $R \to \infty$. The appearance of the maximum of $\Gamma_2$ is not a surprise in the molecular case. From Eq. (3.1) for the atomic case, it follows that $\Gamma \simeq |\varepsilon_0|^{1/2}(\omega-|\varepsilon_0|)^{3/2}$, and the maximum appears at $\varepsilon_0=-\omega/4$. In the case of two ZRP's, the dependence of $\Gamma_2$ on $\varepsilon_2(R)$ is more complex and the maximum appears at a different value of $\varepsilon_2(R)$ For example, if $\omega=7$ eV, the maximum of $\Gamma$ emerges at $R=2.5a_B$ [$\varepsilon(R)=-2.04$ eV].

The analysis of the excited term $\varepsilon_1$ is a more complicated. There are two regions which have to be considered separately: $R \geq R_g$ and $R < R_g$. If $R \geq R_g$, $\varepsilon_1$ is real, the shift $\Delta_1$ decreases and passes through a minimum $\Delta_1(R=7.3a_B)=27.31I/I_A$ eV and than increases to $\Delta_g$, while $\Gamma_1$ increases to $\Gamma_g$. More interesting is the region $R < R_g$ since $\varepsilon_1$ is a complex number there which introduces interesting effects. There are two critical points $R_{-1}=2.065a_B$ and $R_0 \cong R_g = 4.246a_B$ where cusp points (discontinuities of the derivative) of the curves $\Delta(R)$ and $\Gamma(R)$ are noticed (Fig. 6). The appearance of $R_{-1}$ is a consequence of the nonanalyticity of the function $(z_0^2+1)^{1/2}$ in Eq. (3.7). When one photon is emitted, $\mu=-1$, it follows that

$$\mathrm{Re}(z_0^2-\mu)\omega=-\mathrm{Re}(\varepsilon_1)+\omega=0$$

($\mathrm{Re}[\varepsilon_1(R_{-1})]=\omega=3$ eV), and both $U_p$ and $\Delta_1$ can be neglected, since $I \ll I_A$. Therefore, as in the case of one ZRP, the branching points of $(z^2-\mu)^{1/2}$ are the points where the shift and width have jumps. The condition $z^2-\mu=0$ is realized here by change of the internuclear distance $R$. If the frequency is lower, a process with $\mu=-2$ is also possible, and an additional point $R_{-2}$ appears. It is also interesting to note that the total width $\Gamma_1+\Gamma_R$ can either be increased or lowered by the presence of the laser field. From Eq. (3.6) it follows that the transition point for $\Gamma_1$ from a positive to a negative value is defined by the condition

$$\mathrm{Re}(\Delta z)\mathrm{Im}(z_0)+\mathrm{Re}(z_0)\mathrm{Im}(\Delta z)\cong 0 .$$

The critical point $R_0 \cong R_g$ is defined by $\varepsilon_1=0$ and therefore $z_0^2=0$, i.e., $R=R_g$ is the branching point of the function $(z_0^2)^{1/2}$. At this point, the channel for ionization without absorption of photons is closed, and the one-photon ionization becomes the dominant channel.

The discussed approximate and numeric solutions agree completely if $I < 10^{12}$ W/cm$^2$ and $R > 0.5a_B$. This conclusion is valid for any value of the angle between $\hat{\mathbf{R}}$ and $\hat{\mathbf{k}}$ (within the range $g \ll 1$, see Appendix C). Figures 7 and 8 show the numerically calculated shifts and widths $\Delta_1$, $\Delta_2$, $\Gamma_1$, and $\Gamma_2$, for the laser field of intensity $I=10^{-6}I_A$. Here the approximate and exact solutions agree to within 1%, except for small $R$, as was discussed earlier in this section. Each of the results is given for three values of the frequency $\omega=1$, 2, and 3 eV. The maxima of the shifts and widths are largest for the lowest frequency. This is a consequence of the inverse dependence of parameters $B$ and $a$ on $\omega$. When $\omega$ increases, the position of the critical point $R_{-1}$ [where $\mathrm{Re}\varepsilon_1(R_{-1})=\omega$] is shifted toward the smaller values of $R$, since $\varepsilon_1(R) > \varepsilon_1(R')$ as $R < R'$. The position of the second critical point $R \cong R_g$ is independent of frequency. It can also be noticed that the position of the minimum of $\Delta_2$ and maximum of $\Gamma_2$ are shifted toward smaller $R$ with the in-

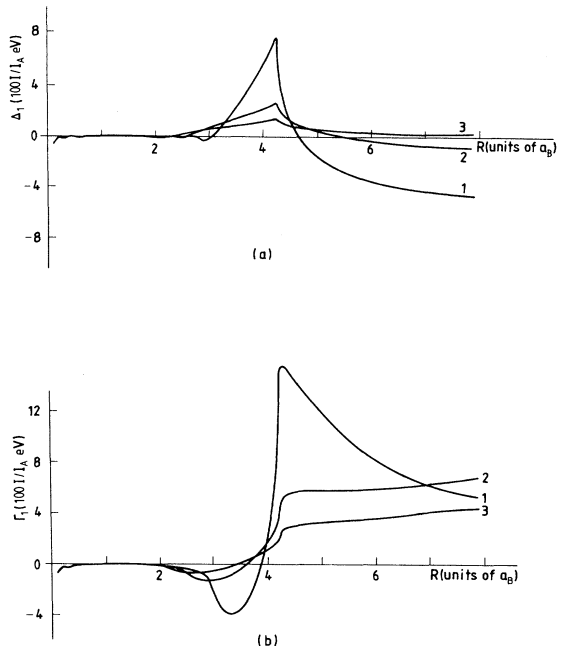


FIG. 7. (a) Scaled shift $\Delta_1$ and (b) width $\Gamma_1$ of the excited electronic term of the $H_2^-$ ion, calculated at the laser field of intensity $I=10^{-6}I_A$, for different photon frequencies $\omega=1$, 2, and 3 eV.

crease of the frequency. Since $|\varepsilon_2|$ decreases when $R$ increases, the condition $|\varepsilon_2|=\omega$ is reached at smaller $R$ if $\omega$ is higher (Fig. 8).

When $I>10^{13}$ W/cm$^2$, the numerical results are significantly different from the approximate ones, which means that the contribution of the multiphoton processes becomes significant. Figure 9 shows the results for the $H_2^-$ system at $I=10^{13}$ W/cm$^2$ and $\omega=3$ eV. The onset of $\Gamma_2$ is at smaller values of $R$ if the field is stronger than the approximate result gives. Besides, the absolute values of the extremes of $\Gamma_2$ and $\Delta_2$ are smaller and are shifted towards larger $R$. Figure 10 shows the results for the $OH^-$ ion. The binding energies of the $H^-$ and $O^-$ ion are 0.7542 and 1.462 eV, respectively, and $R_g(OH^-)=3.6a_B$. The qualitative behavior of the widths and the shifts for this system is approximately the same as that for the $H_2^-$ system (relative positions of the maxima and minima and critical points are approximately the same). $\Delta_{2g}$ and $\Gamma_{2g}$ for this case are

$$\Delta_{2g}=-31I/I_a \text{ eV} ,$$
$$\Gamma_{2g}=382I/I_A \text{ eV} . \tag{3.11}$$

As a consequence, there is a crossing of $\Gamma_1$ and $\Gamma_2$ at large $R$ and $\Delta_2$ tends to negative values.

Figure 11 shows the total width and the real part of $\varepsilon_{-1}$ with and without the laser field versus $R$, in the vicinity of $R_g$, at $\omega=3$ eV and $I=2\times10^{-3}I_A$. The total width of $\varepsilon_1$ is lowered by the presence of the field as a consequence of the negative value of $\Gamma_1$. This is true for those $R$ that are smaller than the value which approximately satisfies the equation

$$\mathrm{Re}(\Delta z)\mathrm{Im}(z_0)+\mathrm{Re}(z_0)\mathrm{Im}(\Delta z)\cong 0 .$$

Crossing of the term $\mathrm{Re}\varepsilon_1+\Delta_1-U_p$ with the continuum edge corresponds to the point of nonanalyticity of the function $(z^2)^{1/2}$, i.e., to the closing of the ionization channel which takes place without any photon emission (absorption). This corresponds to the jump of $\Gamma_R+\Gamma_1$ in Fig. 11(b). Therefore, the presence of a laser can increase the stability of a negative quasimolecular ion in the range of internuclear distances $R<R_g$.

Finally, Figs. 12 and 13 represent the widths and shifts of the molecular terms as functions of the laser intensity at fixed $R$. As in the case of one ZRP, the critical points that correspond to the closing of subsequent ionization channels can be noticed. These points appear at intensities for $\Delta_1$ and $\Gamma_1$ which differ from those for $\Delta_2$ and $\Gamma_2$. In the case of higher frequencies, the branching points of $(z^2-1)^{1/2}$ appear at higher intensities. The depths of $\Delta$ and $\Gamma$ are better pronounced in the atomic case since the term $J(\bar{\varepsilon},R)$ on the right-hand side of Eq. (2.11) smooths the curves. We note that the critical points for larger $R$ appear at higher intensities which is in agreement with the condition

$$[U_p-\Delta_2+|\varepsilon_2(R)|-\omega]^{1/2}=0 ,$$

since $|\varepsilon_2(R')|<|\varepsilon_2(R)|$ for $R'>R$.

## IV. CONCLUSIONS

The analysis of the numerical solution of the eigenvalue equation (2.11) for the widths and ac Stark shifts of the excited quasimolecular term $|1\rangle$ and the ground-state term $|2\rangle$, in the presence of a circularly polarized laser field, yields the following conclusions.

(i) The closing of the channel for a $\mu$-photon ionization of a quasimolecular term is determined by the condition $\mathrm{Re}(z_i^2-\mu)=0$, $i=1,2$. In the atomic case ($\mu=1,2,\ldots$), this condition was reached by changing the laser intensity. In the molecular case this is achieved by changing both $R$ and the intensity. In the considered examples, if $R<R_g$ then $\mu=-1,0,1,\ldots$, i.e., the ionization is also possible with simultaneous emission of photons into the field. Therefore, for a range of $R$, the total ionization width $\Gamma_1+\Gamma_R$ may be smaller than the original one ($\Gamma_R$, in absence of the field). Thus, the ionization rate of a quasimolecular ion is suppressed by presence of a laser field (for $R<R_g$). It is also noticed that the total shifts of the excited term, induced by both $U_p$ and ac Stark shift, decreases the critical internuclear distance $R_g$ at which the excited term of negative quasimolecular ion enter its ionization continuum. This further decreases the collisional ionization rate of the quasimolecule.

(ii) $\Delta_2$ and $\Gamma_2$ have minima and maxima, respectively, at certain values of $R$. The former shows the possibility of increasing the depth of potential well in the ground state of molecule by the presence of a laser field.

(iii) Shifts and widths of the terms are larger for lower frequencies.

(iv) In the case of low laser intensities ($I<10^{12}$

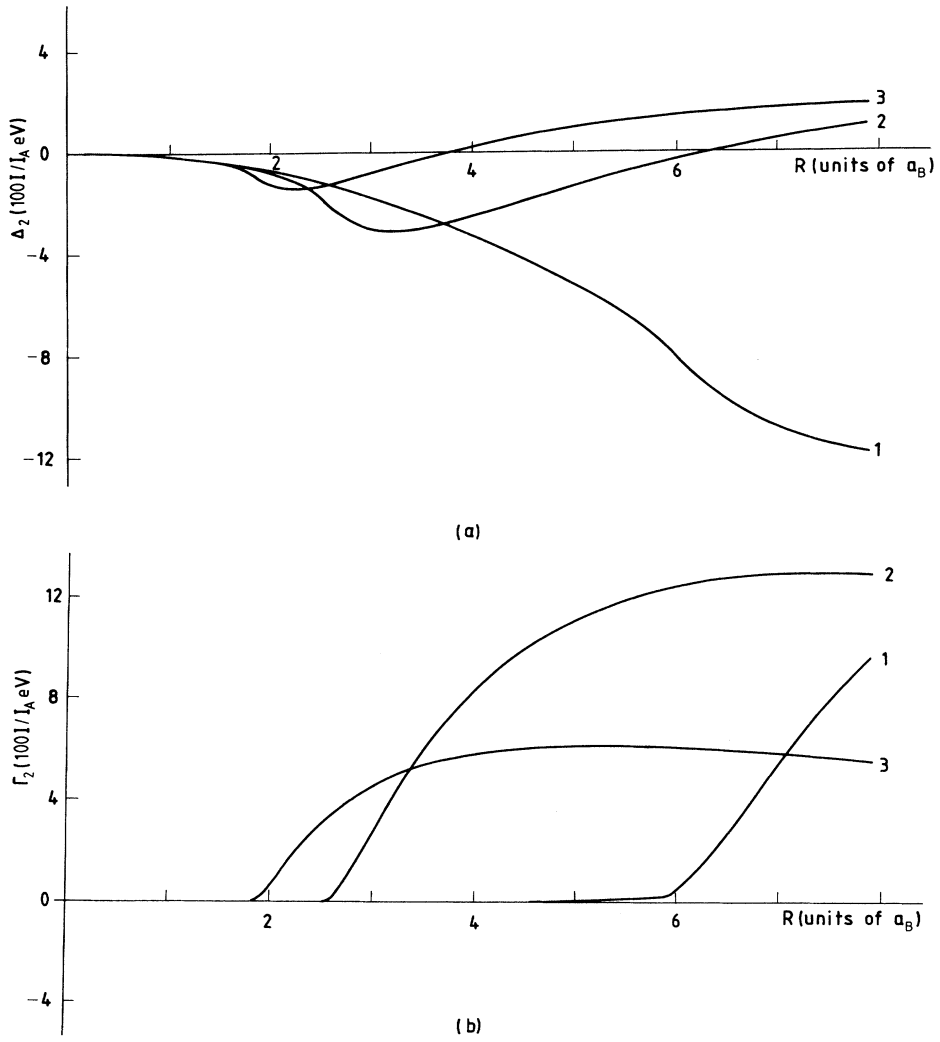


FIG. 8. (a) Scaled shift $\Delta_2$ and (b) width $\Gamma_2$ of the lower electronic term of the $H_2^-$ ion, calculated at the laser field of intensity $I=10^{-6}I_A$, for different photon frequencies $\omega=1$, 2, and 3 eV.

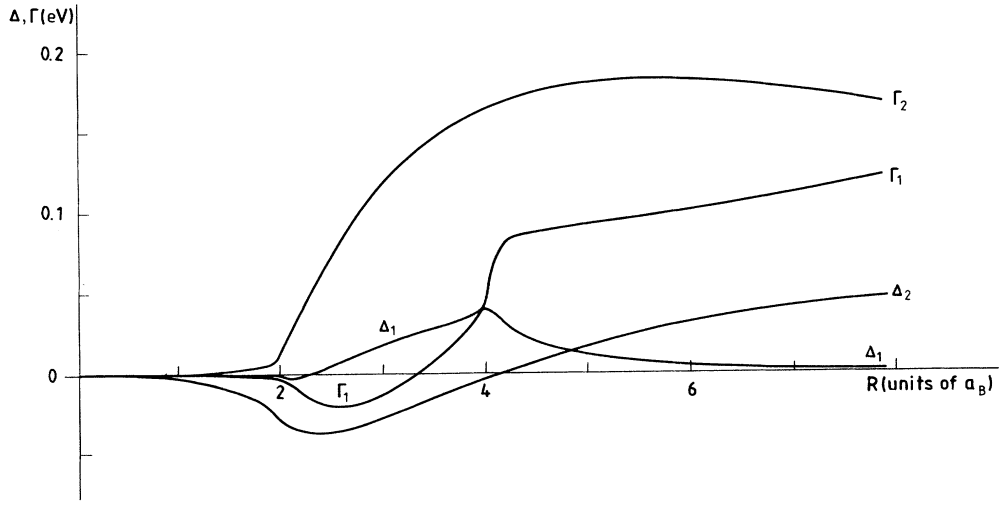


FIG. 9. Shifts $\Delta$ and widths $\Gamma$ of the electronic terms of the $H_2^-$ ion, induced by the laser field of intensity $I=10^{13}$ W/cm$^2$ and frequency of $\omega=3$ eV. The ponderomotive potential is $U_p=0.16$ eV.

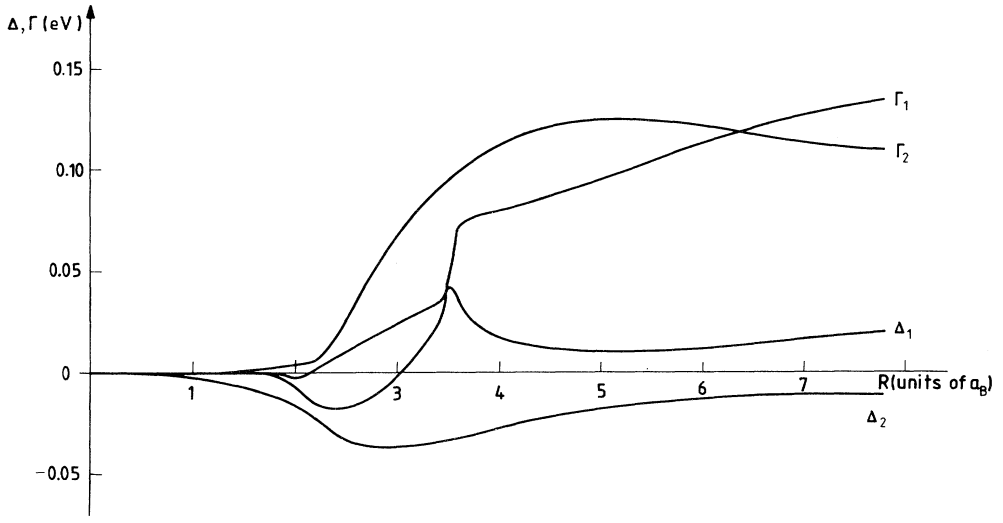


FIG. 10. Shifts Δ and widths Γ of the electronic terms of the $OH^-$ ion, induced by the laser field of intensity $I=10^{13}$ W/cm$^2$ and frequency of $\omega=3$ eV. The ponderomotive potential is $U_p=0.16$ eV.

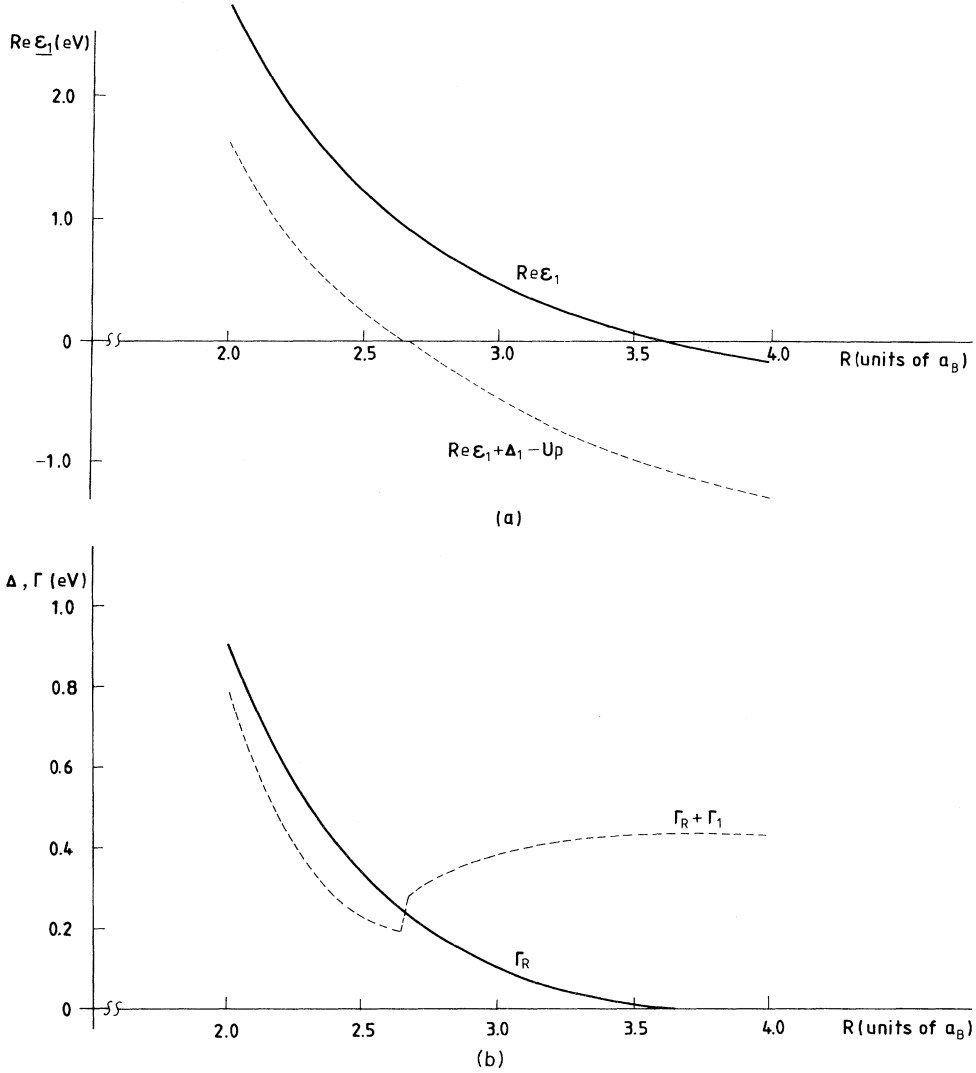


FIG. 11. Excited electronic term of (a) the $OH^-$ ion and (b) its width in the absence (solid line) and in the presence of the laser field (dashed line) of intensity $I=2\times10^{-3}I_A$ and frequency $\omega=3$ eV, in the vicinity of the critical distance $R_g$.

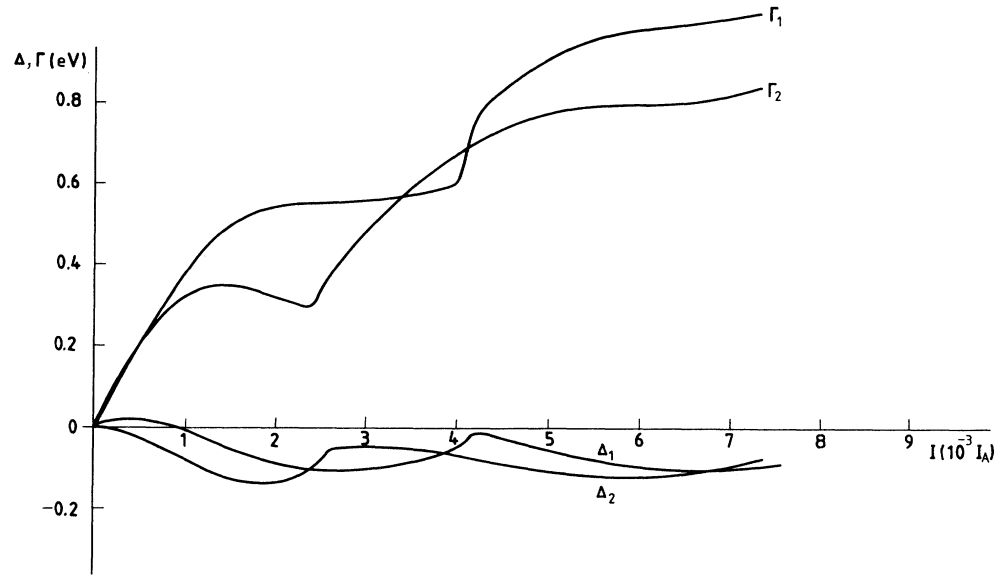


FIG. 12. Shifts and widths of electronic term of the $OH^-$ ion vs the laser-field intensity at fixed internuclear distance $R=6a_B$; $\omega=3$ eV.

W/cm$^2$), one-photon processes are dominant (if energetically allowed), and significant decay of the ground state occurs only when $R$ is such that $|\varepsilon_2(R)|<\omega$. At higher laser intensities, this condition is weakened by intense multiphoton processes.

(v) As $R\to\infty$, $\Delta_j$ and $\Gamma_j$ $(j=1,2)$ tend to the limiting values which can be obtained as the solutions of the problem with one ZRP. In that limit the potentials become independent.

(vi) The quantities $\Delta_j$ and $\Gamma_j$ as functions of the intensity $I$ increase linearly if $I\ll I_A$. With the further increase of $I$, effects similar to those in the case of one ZRP appear: nonlinearity and closure of the channels for a $\mu$-photon absorption.

(vii) When the internuclear distance tends to zero, the model of two-ZRP treated here needs to be redefined, by introduction of a parameter of the interaction between the potentials. Then, in the limit $R\to 0$, the two-ZRP tends to the one with equivalent strength given by Eq. (B9), which corresponds to the united-atom limit of a real quasimolecular system.

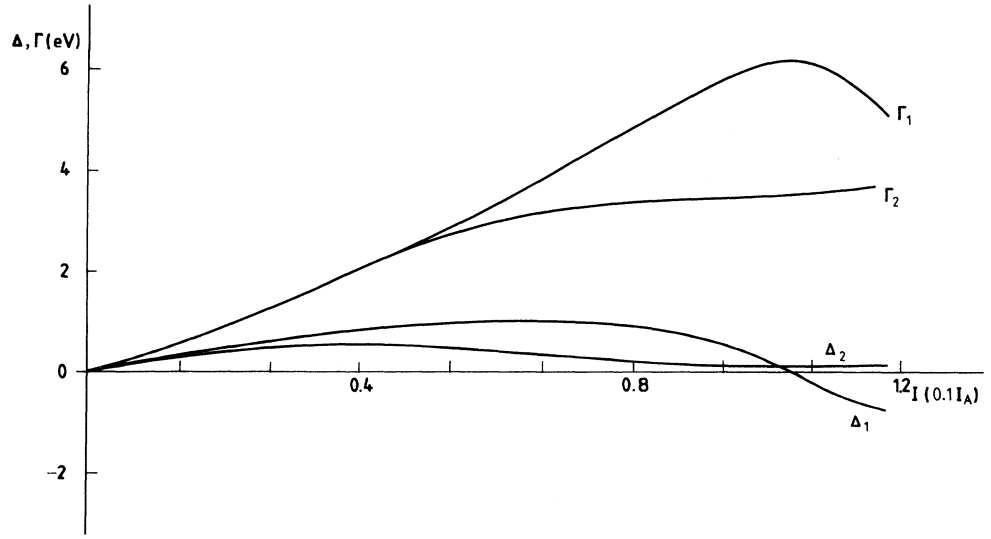


FIG. 13. Shifts and widths of electronic term of the $OH^-$ ion vs the laser-field intensity at fixed internuclear distance $R=6a_B$; $\omega=10$ eV.

## ACKNOWLEDGMENTS

This work was partially supported by the U.S. National Science Foundation and Science Foundation of Serbia through the U.S.-Yugoslav Joint Board of Scientific and Technological Cooperation under Contract No. NSF801.


## APPENDIX A

In this appendix, the explicit expressions for the nonrelativistic Volkov Green's operator are derived. These are used in Sec. II. The time-dependent retarded Green's operator $G_L^{(+)}(t,t')=G_L(t,t')$ is defined by [22]

$$\left[i\frac{\partial}{\partial t}-H_L\right]G_L(t,t')=1\delta(t-t') \tag{A1}$$

with the initial condition $G_L(t,t')=0$ if $t<t'$. $H_L$ is the electron Hamiltonian in the laser field, $H_L=\omega a^\dagger a+(\mathbf{p}+e\,\mathbf{A})^2/(2m)$ in the momentum gauge. In QED formalism, $G_L$ can be written in the form

$$\begin{aligned} G_L(t,t')&=G_L(t-t')\\ &=-i\vartheta(t-t')\sum_\nu d\mathbf{q}|K_{N-\nu,\mathbf{q}}\rangle\langle K_{N-\nu,\mathbf{q}}|\\ &\quad\times\exp[-iz(t-t')]\ ,\\ z&=E_{N-\nu,q}-i\varepsilon\ ,\\ \varepsilon&\to 0^+\ ,\\ E_{N-\nu,q}&=(N-\nu)\omega+E_q+U_p\ , \end{aligned} \tag{A2}$$

where $|K_{N-\nu,\mathbf{q}}\rangle$ is the stationary Volkov solution of the Schrödinger equation

$$H_L|K_{N-\nu,\mathbf{q}}\rangle=E_{N-\nu,q}|K_{N-\nu,\mathbf{q}}\rangle \tag{A3}$$

and where $E_q=q^2/(2m)$ and $U_p=e^2A_0^2/(4m)$ are kinetic energy of the electron and the laser ponderomotive potential, respectively. Using the generalized Bessel functions [16] $\gamma_\mu=\gamma_\mu(\delta^{(1)},\delta^{(2)},\eta)$, where the parameter $\eta$ and $\delta^{(j)}$, $j=1,2$ are defined by

$$\begin{aligned} \eta&=\frac{\cos(2\kappa)}{2\omega}U_p\ ,\\ \delta^{(j)}&=\alpha_0\mathbf{\Lambda}_j\cdot\mathbf{q}\ ,\\ \alpha_0&=eA_0/(m\omega)\ , \end{aligned} \tag{A4}$$

the Volkov solution can be written in the form

$$|K_{n-\nu,\mathbf{q}}\rangle=\sum_\mu\gamma_\mu|N+\mu-\nu,\mathbf{q}-\mu\mathbf{k}\rangle\ . \tag{A5}$$

Introducing a complete set of vectors $\{|\vartheta\rangle\}$, so that

$$\begin{aligned} &\langle\vartheta|\nu\rangle=(2\pi)^{-1/2}\exp(i\nu\vartheta)\ ,\\ &\langle\vartheta|\vartheta'\rangle=\delta(\vartheta-\vartheta')\ ,\\ &\int_0^{2\pi}d\vartheta|\vartheta\rangle\langle\vartheta|=1 \end{aligned} \tag{A6}$$

(the phase representation [23]), one obtains

$$\begin{aligned} K_{N-\nu,\mathbf{q}}(\mathbf{r},\vartheta)&=\langle\vartheta,\mathbf{r}|K_{N-\nu,\mathbf{q}}\rangle\\ &=(2\pi)^{-2}\sum_\mu\gamma_\mu\exp[i(\mathbf{q}-\mu\mathbf{k})\cdot\mathbf{r}+i(N-\nu+\mu)\vartheta]\\ &=(2\pi)^{-1/2}\exp\{i[\mathbf{q}\cdot\mathbf{r}+(N-\nu)\vartheta+\alpha_0\mathbf{q}\cdot(\mathbf{\Lambda}_1\sin\varphi+\mathbf{\Lambda}_2\cos\varphi)+\eta\sin(2\varphi)]\}\ , \end{aligned} \tag{A7}$$

where $\varphi=\mathbf{k}\cdot\mathbf{r}-\vartheta$. From Eq. (A2), the time-independent Green's operator $G_L(E)=(E-H_L+i\varepsilon)^{-1}$, $\varepsilon\to 0^+$ is obtained as

$$G_L(E)=\int_{-\infty}^{+\infty}dt\ G_L(t)e^{iEt-\varepsilon t}=\sum_\nu\int d\mathbf{q}\frac{|K_{N-\nu,\mathbf{q}}\rangle\langle K_{N-\nu,\mathbf{q}}|}{E+i\varepsilon-E_{N-\nu,q}}\ , \tag{A8}$$

$G_L(E)$ satisfies the outgoing-wave boundary conditions. In the coordinate-phase representation, using Eq. (A7) and the integral (which corresponds to the divergent waves)

$$\frac{1}{(2\pi)^4}\int d\mathbf{q}\frac{\exp[i\mathbf{q}\cdot(\mathbf{r}-\mathbf{r}'-\mathbf{f})]}{E+i\varepsilon-E_{N-\nu,q}}=-\frac{m}{(2\pi)^2}\frac{\exp[ik_\nu|\mathbf{r}-\mathbf{r}'-\mathbf{f}|]}{|\mathbf{r}-\mathbf{r}'-\mathbf{f}|}\ , \tag{A9}$$

one obtains

$$\begin{aligned} G_L(E;\mathbf{r},\vartheta;\mathbf{r}',\vartheta')&=\langle\mathbf{r},\vartheta|G_L(E)|\mathbf{r}',\vartheta'\rangle\\ &=-\frac{m}{(2\pi)^2}e^{i\phi}\sum_\nu e^{i(N-\nu)(\vartheta-\vartheta')}\frac{\exp[ik_\nu|\mathbf{r}-\mathbf{r}'-\mathbf{f}|]}{|\mathbf{r}-\mathbf{r}'-\mathbf{f}|}\ , \end{aligned} \tag{A10}$$

where

$$\phi=\phi(\mathbf{r},\vartheta;\mathbf{r}',\vartheta')=\eta[\sin(2\varphi)-\sin(2\varphi')],\quad \varphi'=\mathbf{k}\cdot\mathbf{r}'-\vartheta' ,$$
$$\mathbf{f}=\mathbf{f}(\mathbf{r},\vartheta;\mathbf{r}',\vartheta')=\alpha_0\{\mathbf{\Lambda}_1[\sin(\varphi')-\sin(\varphi)]+\mathbf{\Lambda}_2[\cos(\varphi')-\cos(\varphi)]\} , \tag{A11}$$
$$k_\nu^2=2m\,[E-U_p-(N-\nu)\omega] .$$

Starting from Eqs. (A2) and (A3), with the addition of the Poisson summation formula [24]

$$\sum_\nu \int_{-\infty}^{+\infty} dx\, g(x)e^{-i\nu x}=2\pi\sum_\nu g(2\pi\nu) \tag{A12}$$

and the integral

$$\int d\mathbf{q}\exp\left[i\mathbf{q}\cdot(\mathbf{r}-\mathbf{r}'-\mathbf{f})-i\frac{q^2}{2m\omega}(\vartheta-\vartheta')\right]=\left[\frac{2\pi m\omega}{i(\vartheta-\vartheta')}\right]^{3/2}\exp\left[i\frac{m\omega}{2(\vartheta-\vartheta')}(\mathbf{r}-\mathbf{r}'-\mathbf{f})^2\right] . \tag{A13}$$

$G_L$ can also be obtained in the form

$$G_L(E;\mathbf{r},\vartheta;\mathbf{r}',\vartheta')=-\frac{i}{\omega}\sum_\nu \vartheta(\tau_\nu)\left[\frac{m}{2\pi i\tau_\nu}\right]^{3/2}\exp\left[i\left[\tau_\nu(E-U_p)+\phi+\frac{m}{2\tau_\nu}(\mathbf{r}-\mathbf{r}'-\mathbf{f})^2\right]\right] , \tag{A14}$$

where $\omega\tau_\nu=\vartheta-\vartheta'+2\pi\nu$.

Finally, we state one more useful formula which is also used in Sec. II, in connection with the $3D$ delta-function potentials. This is

$$\lim_{r\to 0} G_L(E;\mathbf{r},\vartheta;\mathbf{0},\vartheta')=-\frac{m}{(2\pi)^2}\frac{\exp[i\phi(\vartheta,\vartheta')]}{f(\vartheta,\vartheta')}\sum_\nu \exp[i(N-\nu)(\vartheta-\vartheta')]\exp[ik_\nu f(\vartheta,\vartheta')]-1\}$$
$$-\frac{m\delta(\vartheta-\vartheta')}{2\pi r|\hat{\mathbf{r}}+\alpha_0 k\hat{\mathbf{k}}\cdot\hat{\mathbf{r}}[\mathbf{\Lambda}_1\cos(\vartheta)+\mathbf{\Lambda}_2\sin(\vartheta)]|} , \tag{A15}$$

where

$$\phi(\vartheta,\vartheta')=-2\eta\sin(\vartheta-\vartheta')\cos(\vartheta+\vartheta') , \tag{A16a}$$
$$f(\vartheta,\vartheta')=2\alpha_0\left|\sin\left[\frac{\vartheta-\vartheta'}{2}\right]\right|\left[\cos^2(\kappa)\cos^2\left[\frac{\vartheta+\vartheta'}{2}\right]+\sin^2(\kappa)\sin^2\left[\frac{\vartheta+\vartheta'}{2}\right]\right]^{1/2} . \tag{A16b}$$

## APPENDIX B

It is easy to show that the problem of two ZRP's in a laser field is correctly defined in the case when the inter-potential distance increases to infinity. When $R\to\infty$, it follows that

$$\lim_{R\to\infty} S_{\mu\nu}(\tilde{E};\mathbf{R}_1,\mathbf{R}_2)=0 ,$$
$$\kappa_j b_{j\mu}+\sum_\nu F_{\mu\nu}(\tilde{E})b_{j\nu}=0,\quad j=1,2 \tag{B1}$$

and so the problem transforms into two independent problems for each of the ZRP in the system. But, when $R\to 0$, the two ZRP's overlap and the problem of the divergence of $S_{\mu\nu}(\tilde{E};\mathbf{R}_1,\mathbf{R}_2)$ appears. This problem occurs even in the absence of the laser field. In that case, the energy equation is of the form (1.15), and the term on the right-hand side of that equation is singular as $R\to 0$. For example, if $\kappa_1=\kappa_2$, then $\kappa=\kappa_1\pm\exp(-\kappa R)/R$ and the quasienergy $\varepsilon\simeq -1/R^2\to-\infty$ a $R\to 0$. The problem is usually treated [8] by assuming that the ZRP depth depends upon $R$ and that $\kappa_j(R)=\alpha_j(R)-1/R$, where $\alpha_j(R)$ is a limited function of $R$, for all $R$'s. Here we shall follow another, more physical, approach based on the idea of connecting the strength of the "united" ZRP with those of the separated ZRP's. Indeed, when $R\to 0$, the two ZRP's are not independent any more and one needs to define their interaction (correlation). The boundary conditions (2.2) with $r_1\to 0$ when $R\to 0$ mean that simultaneously $r_2\to 0$ and vice versa. That means that the term with $\delta(\mathbf{r}_1)$ in (2.1) should be somehow connected with $\delta(\mathbf{r}_2)$, but in the same time that these are decoupled when $R\neq 0$. Having that in mind, the potential $V$ of the two ZRP's is redefined as

$$V(\mathbf{r},\mathbf{R})|_{R\to 0}=\frac{2\pi}{m}\frac{1}{\kappa_1\kappa_2-f_1f_2}$$
$$\times\sum_{i=1,2}[\kappa_{3-i}\delta(\mathbf{r}_i)+f_i\delta(\mathbf{r}_{3-i})]\frac{\partial}{\partial r_i}r_i \tag{B2}$$

introducing auxiliary functions $f_i$ which define the interaction of the two ZRP's when $R\to 0$. Boundary conditions (2.2) can be now written in the form

$$\lim_{\substack{r_i\to 0 \\ (\text{i.e.},\, r_{3-i}\to 0,\, R\to 0)}} |\Psi_{\tilde{E}}(\mathbf{r},\mathbf{R})\rangle = \left[\frac{1}{r_i}-\kappa_i\right]|B_i\rangle + D(\beta;\mathbf{R}_i,\mathbf{R}_{3-i})|B_{3-i}\rangle \ , \quad \text{(B3)}$$

where $D$ is an operator in photon space defined as

$$D|B_i\rangle = f_i|B_i\rangle, \quad f_i|_{R\geq R_c}=0 \ . \quad \text{(B4)}$$

$\beta$ is the parameter of the transition between the ZRP. If $R\geq R_c$, Eqs. (B3) and (B4) are equivalent to the equations without the correction. On the other hand, if $R<R_c$, the functions $f_i$ (i.e., the operator $D$) should be chosen to avoid the singularity of the eigenenergy equation when $R=0$. The singularity comes from the terms $S_{\mu\nu}$. Generally, $D$ can be defined so that the equation preserves the same form, and with $k_\nu(\tilde{E})$ replaced with an interaction parameter $\beta_\nu$. If $\beta_\nu=\beta$ for each $\nu$, than $D_{\mu\nu}=\langle N-\mu|D|N-\nu\rangle$ can be written in the form

$$D_{\mu\nu}=\frac{1}{2\pi}\int_0^{2\pi} d\vartheta \exp[i(\mu-\nu)\vartheta] \times \frac{\exp(i\phi-\beta|\mathbf{R}_1-\mathbf{R}_2-\mathbf{f}|)}{|\mathbf{R}_1-\mathbf{R}_2-\mathbf{f}|} \quad \text{(B5a)}$$

and

$$D_{\mu\nu,\text{cir}}|_{g\ll 1}=\delta_{\mu\nu}D(\beta,\mathbf{R}) \ , \qquad D(\beta,\mathbf{R})=\frac{\exp[-\beta h(0,\mathbf{R})]}{h(0,\mathbf{R})}, \quad g\ll 1 \ , \quad \text{(B5b)}$$

where $h(0,\mathbf{R})$ is given by (2.7c). Using (2.2c), (B4), and (B5b), one gets $f_i=\exp(-\beta h)/h$ and $\lim_{R\to 0} f_i = 1/h-\beta$. In Eqs. (2.4) and (2.8a) for the quasienergy, the required correction is $S_{\mu\nu}\to S_{\mu\nu}-D_{\mu\nu}$, i.e., $S\to S-D$. As a consequence, there is no more singularity as $R\to 0$ but, for $R\geq R_c$, the results are unchanged. For Eq. (2.11), the correction is of the form $J\to J-d$, where

$$d(\tilde{\varepsilon},\mathbf{R})=\exp[-\beta R f(0,\mathbf{R})]/f(0,\mathbf{R}) \ , \qquad f^2(0,\mathbf{R})=1+a\sin^2 b \ . \quad \text{(B5c)}$$

Equation (2.8a), with the correction included, becomes

$$[\kappa_1+F(\tilde{\varepsilon})][\kappa_2+F(\tilde{\varepsilon})] = [S(\tilde{\varepsilon},\mathbf{R})-D(\beta,\mathbf{R})][S(\tilde{\varepsilon},-\mathbf{R})-D(\beta,-\mathbf{R})] \ . \quad \text{(B6)}$$

Using the formula

$$\lim_{R\to 0}[S(\tilde{\varepsilon},\mathbf{R})-D(\beta,\mathbf{R})]=F(\tilde{\varepsilon})+\beta \ , \quad \text{(B7)}$$

where $F(\tilde{\varepsilon})$ is given by (2.8b), Eq. (B6), in the limit $R\to 0$ takes the form

$$\frac{\kappa_1\kappa_2-\beta^2}{\kappa_1+\kappa_2-2\beta}+F(\tilde{\varepsilon})=0 \ , \quad \text{(B8)}$$

which corresponds to the equation for one ZRP in a laser field, $\kappa+F(\tilde{\varepsilon})=0$. Therefore, when $R\to 0$, the two-ZRP tend to the one with equivalent strength

$$\frac{2\pi}{m}\frac{1}{\kappa}=\frac{2\pi}{m}\frac{\kappa_1+\kappa_2-2\beta}{\kappa_1\kappa_2-\beta^2} \ . \quad \text{(B9)}$$

When the interaction parameter $\beta\to 0$, it follows that

$$\frac{1}{\kappa}=\frac{1}{\kappa_1}+\frac{1}{\kappa_2} \ . \quad \text{(B10)}$$

In the absence of the laser field singularity $R\to 0$, in Eq. (1.11) can be avoided similarly as in (B2), introducing the interaction functions $f(R)=\exp(-\beta R)/R$, for $R<R_c$. Then, instead of (1.11), one gets

$$(\kappa-\kappa_1)(\kappa-\kappa_2)=\{[\exp(-\kappa R)-\exp(-\beta R)]/R\}^2 \ ,$$

and when $R\to 0$ this yields Eqs. (B9) and (B10).

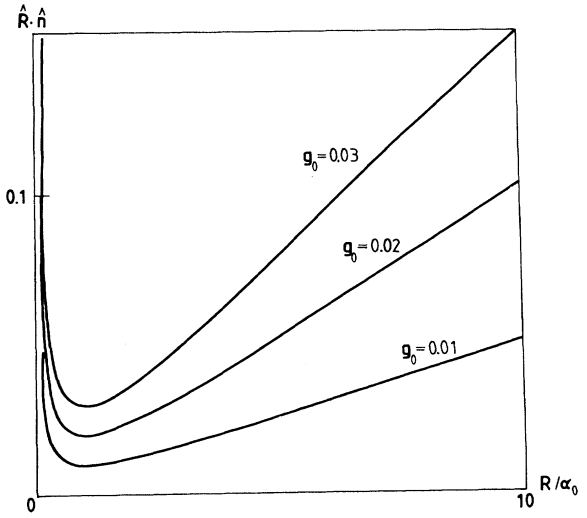


FIG. 14 Parameter $z=\hat{\mathbf{R}}\cdot\hat{\mathbf{n}}$ vs $y=R/\alpha_0$ at fixed $x_0=\sin(\varphi_-)=0.7$. Surfaces below a curve defines the range of validity of approximation $g\leq g_0$.

## APPENDIX C

Here we consider the approximation $g\ll 1$, where $g$ is defined by Eq. (2.7d). The function $g$ can be written in the form

$$g=g(x,y,z)=2^{5/2}\frac{xyz}{y^2+2x^2} \ ,$$

where

$$x=\sin(\varphi_-)\in(-1,1) \ , \qquad y=\frac{R}{\alpha_0}\in(0,\infty) \ , \qquad z=\hat{\mathbf{R}}\cdot\hat{\mathbf{n}}\in(-1,1) \ . \quad \text{(C1)}$$

This function has the following properties: (a) $g=0$ if $\hat{\mathbf{k}}\|\hat{\mathbf{R}}$, i.e., $\hat{\mathbf{R}}\cdot\hat{\mathbf{e}}_1=0=\hat{\mathbf{R}}\cdot\hat{\mathbf{e}}_2$, (b) $g\ll 1$ if $\alpha_0\ll R$, (c) if

$\alpha_0 \cong R$ or $\alpha_0 \gg R$, it follows that $\mathbf{k}\cdot(\mathbf{R}_1 \pm \mathbf{R}_2) \ll 1$ and $\varphi_\pm \cong (\vartheta + \vartheta')/2$ (if $k\alpha_0 \ll 1$), and (d) $g(x,y,z) = -g(-x,y,z) = -g(x,-y,z) = -g(x,y,-z)$. From the last property, it follows that it is sufficient to consider the first octant in the $xyz$ system.

Figure 14 represents curves

$$z(y) = \frac{g_0}{2^{5/2}} \frac{y^2 + 2x_0^2}{x_0 y} \tag{C2}$$

for $g_0 = 0.01$, 0.02, and 0.03 and $x_0 = 0.7$. The surfaces below the curves define the range of applicability of approximation $g \ll 1$.


[1] N. L. Manakov and L. P. Rapoport, Zh. Eksp. Teor. Fiz. **69**, 842 (1975) [Sov. Phys. JETP **42**, 430 (1976)].

[2] I. J. Berson, J. Phys. B **8**, 3078 (1975).

[3] H. G. Muller, A. Tip, and M. J. van der Wiel, J. Phys. B **16**, L679 (1983).

[4] H. G. Muller and A. Tip, Phys. Rev. A **30**, 3039 (1984).

[5] W. Becker, J. K. McIver, and M. Confer, Phys. Rev. A **40**, 6904 (1989).

[6] B. M. Smirnov and O. B. Firsov, Zh. Eksp. Teor. Fiz. **47**, 232 (1964) [Sov. Phys. JETP **20**, 156 (1965)].

[7] Yu. N. Demkov, Zh. Eksp. Teor. Fiz. **46**, 1126 (1964) [Sov. Phys. JETP **19**, 762 (1964)].

[8] Yu. N. Demkov and V. N. Ostrovskii, *Zero Range Potentials and Their Application in Atomic and Molecular Physics* (Plenum, New York, 1988).

[9] A. Grossmann, E. Hoegh-Krohn and M. Mebkhout, J. Math. Phys. **21**, 2376 (1980).

[10] S. Albeverio, R. Hoegh-Krohn and M. Mebkhout, J. Math. Phys. **25**, 1327 (1984).

[11] N. Durante, G. P. Arrighini, and C. Guidotti, Z. Phys. D **8**, 63 (1988).

[12] R. K. Janev, L. P. Presnyakov, and V. P. Shevelko, *Physics of Highly Charged Ions* (Springer-Verlag, Berlin, 1985).

[13] R. Shakeshaft, J. Opt. Soc. Am. B **4**, 705 (1987).

[14] V. A. Esaulov, Ann. Phys. (Paris) **11**, 493 (1986).

[15] Yu. N. Demkov, G. F. Drukarjev, and V. V. Kuchinskii, Zh. Eksp. Teor. Fiz. **58**, 944 (1970).

[16] E. J. Kelsey and L. Rosenberg, Phys. Rev. A **19**, 756 (1979).

[17] I. S. Gradshteyn and I. M. Ryzhik, *Tables of Integrals, Series and Products* (Academic, New York, 1980).

[18] R. M. Potvliege and R. Shakeshaft, Phys. Rev. A **38**, 6190 (1988).

[19] M. Dorr and R. M. Potvliege, Phys. Rev. A **41**, 1472 (1990).

[20] J. I. Gersten and M. H. Mittleman, J. Phys. B **9**, 2561 (1976).

[21] M. Pont, N. R. Walet, and M. Gavrila, Phys. Rev. A **41**, 477 (1990).

[22] R. G. Newton, *Scattering Theory of Waves and Particles* (McGraw-Hill, New York, 1966).

[23] I. Bialinicki-Birula and Z. Bialinicka-Birula, Phys. Rev. A **14**, 1101 (1976).

[24] *Handbook of Mathematical Functions,* edited by M. Abramowitz and I. A. Stegun (Dover, New York, 1972).